CHARACTERIZATION OF THE PHOTOSWITCHABLE FLUORESCENT PROTEIN rsEGFP 2

by

BAYONLE ADESOLA

(Under the Direction of Peter A. Kner)

ABSTRACT

Physicists are using nanoscopic techniques with photo-switchable fluorescent probes to see biological structures beyond the resolution limits of conventional microscopes. These probes can be switched on and off reversibly for many cycles and can be used for non-linear nanoscopic imaging techniques. In this thesis I characterized a photo-switchable probe called rsEGFP2 (reversibly photo-switchable Enhanced Green Fluorescent Protein 2) to know its suitability for the nanoscopic imaging technique, Nonlinear Structured Illumination Microscopy (NLSIM). The switching behavior of rsEGFP2 were measured in U2OS cells in which rsEGFP2-actin was expressed. The switch fatigue, decay time constants and background were measured. A switch fatigue greater than 1100 cycles, a decay time constant of 4.5 ms and a ratio of background to peak intensity of 0. 189 at high laser powers (25 mW) were obtained. The high number of switching cycles, fast time constant, and low background confirm the suitability of rsEGFP2 for NLSIM.

INDEX WORDS: Photo switchable Enhanced Green Fluorescent Fluorescence microscopy, structured illumination, fluorescent proteins, switch fatigue, reversible Proteins 2

CHARACTERIZATION OF THE PHOTOSWITCHABLE FLUORESCENT PROTEIN rsEGFP 2

by

BAYONLE ADESOLA

BS, Olabisi Onabanjo University, Ago-Iwoye, Nigeria,2013

A Thesis Submitted to the Graduate Faculty of The University of Georgia in Partial Fulfillment of the Requirements for the Degree

MASTER OF SCIENCE

ATHENS, GEORGIA

2023

CHARACTERIZATION OF THE PHOTOSWITCHABLE FLUORESCENT PROTEIN

rsEGFP 2

by

BAYONLE ADESOLA

Major Professor:	Peter A. Kner
Committee:	Mark Haidekker
	Daichi Kamiyama

Electronic Version Approved:

Ron Walcott
Dean of the Graduate School
The University of Georgia
May 2023

DEDICATION

I dedicated this master's thesis to the glory of God.

ACKNOWLEDGEMENTS

First, I want to offer my unquantifiable gratitude for the meritorious support from my major supervisor, Dr. Peter A. Kner whose priceless advice, guidance, patience, and emotional intelligence has been helpful. I also want to offer immeasurable appreciation to my committee members: Dr. Daichi Kamiyama whose lab provided us with samples for performing experiment and Dr. Mark Haidekker whose class in Biomedical Imaging and Advanced Image Imaging provided me with a strong pedestal to understanding image processing. I am also using this auspicious opportunity to appreciate my family (my mum, brother, and late dad) for all their unflinching support during my journey from high school to graduate school. Finally, I would like to thank all my fellow colleagues at Kner Lab (Yang, Ruizhe, Rachel,Bingxi,Shao and Ming) for all their wonderful help.

TABLE OF CONTENTS

Page

LIST OF TABLES

Page

LIST OF FIGURES

Page

Chapter One

Overview of Fluorescence Microscopy

1.1 Introduction

As physicists observe planetary bodies such as the sun, moon, and the stars to help them understand their physical properties, so do biologists and chemists also observe the behavior of proteins to provide explanations to the enigmatic events in life science. Because the resolution of the human eye is limited to about 100 microns, scientists and physicists depend on tools to view objects on the macroscopic and microscopic scale. Initially, simple telescopes were invented for seeing celestial bodies far away [1]. Simple microscopes followed. Further developments involved the combination of the Objective lens and the Eye piece lens to make the first compound microscopes [2]. A brief history of key discoveries in light microscopy from 1611 to 1994 is shown in Table 1-1 [3].

The compound microscope uses the scattering properties of light to observe features in living cells. Two popular types of compound microscopes (schematics shown in Figure 1-1a [3]) are the dark-field and the bright field microscopes. In the dark-field microscopes the cell is bright relative to a dark background. This is because the rays of light are controlled so that only scattered light enters the microscope lenses. On the other hand, in the bright-field microscope the cell is dark relative to a white background. Again, the image in this case is obtained via simple transmission of light through the cell. Other complicated forms of microscopes using the properties of light are phase-contrast and differential-interference contrast microscopes. These

two microscopes provide contrast between a region of interest and the background using changes in the phase of light and constructive/destructive interference of light as it travels between region of different refractive indexes.

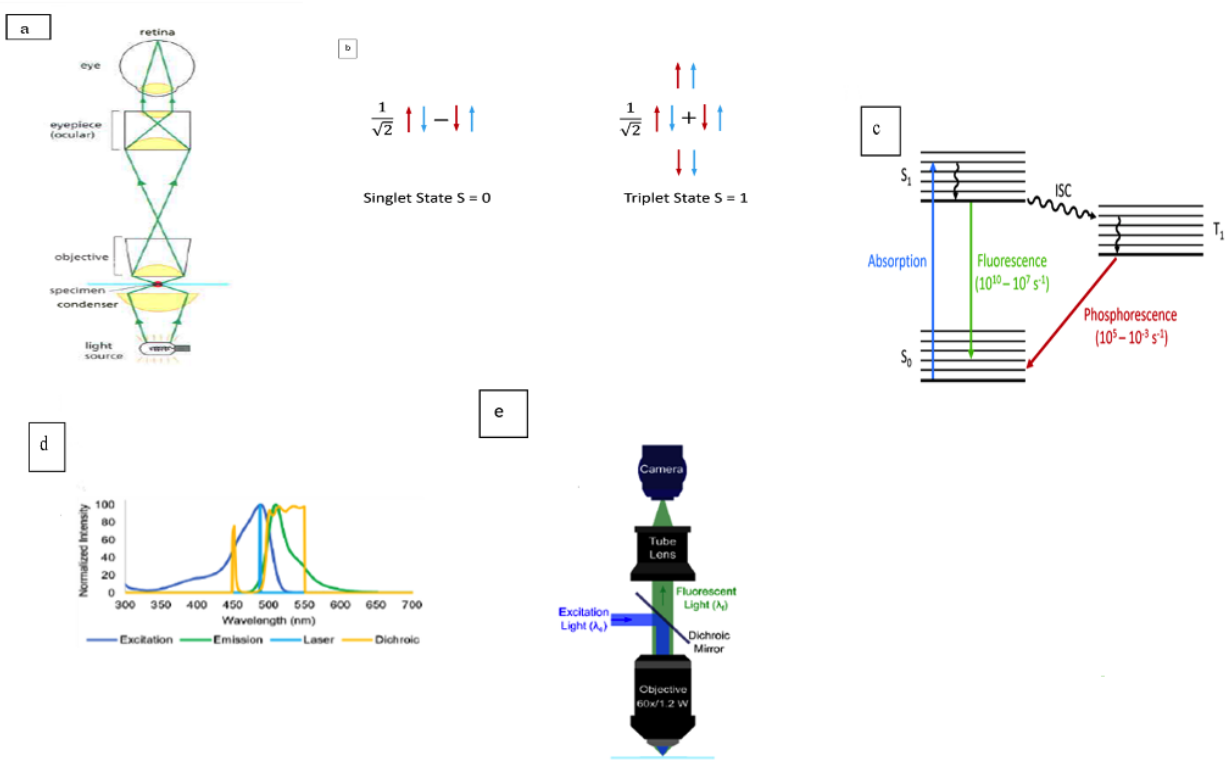

Figure 1-1. Brief details of fluorescence microscopy, fluorescence spectrum and spin states. (a) , Schematics showing the lights paths in a compound microscope. Lights is focused on the sample by the condenser lens & a combination of objective and eye piece lenses enable the image of the sample to be seen by an observer. (b) , Spin states of electrons. (c) , Jablonski diagram showing what happens at the singlet states (S_1, S_0) and Triplets states(T_1) . (d) , Spectrum of Green Fluorescent proteins. (e) , Basics of fluorescence microscope.

Table 1-1[3]. Brief history of microscopy from the discovery of compound microscope to the advents of fluorescence microscopy through discovery of markers (GFP) .

YEAR	DISCOVERIES
1611	**Kepler** suggests a way of making a **compound microscope.**
1655	**Hooke** uses a compound microscope to detect small pores in sections of cork he calls "cells".
1833	**Brown** publishes his microscope observations of orchid, clearly describing the cell nucleus.
1876	**Abbe** analyzes the effects of diffraction on image formation in microscope and shows how to optimize microscope design.
1881	**Retzius** describes many animal cells with a detail that has not been surpassed by any other light microscopist. During the next two decades he, **Cajal** and other histologists develop staining methods and lay the foundations of microscopic anatomy.
1882	**Koch** uses aniline dyes to stain microorganisms and identifies the bacteria that cause tuberculosis and cholera. In the following two decades, other bacteriologist, such as **Klep** and **Pasteur**, identify the preparations under the microscope.
1886	**Zeiss** makes a series of lenses, to the design of **Abbe**, that enable microscopists to resolve structures at the theoretical limits of visible light.
1898	**Golgi** first sees and describe the **Golgi** apparatus by staining cells with silver nitrate.
1930	**Lebedeff** designs and builds the first interference microscope.
1932	**Zernicke** invents the phase contrasts microscope. The developments in 1930 and 1932 allow unstained living cells to be seen in detail for the first time.
1941	**Coons** uses antibiotics coupled to fluorescent dyes to detect cellular antigens.
1952	**Normaski** devises and patents the system of differential interference for light microscope that still bears his name.
1968	**Petran** and collaborators make first confocal microscope.
1981	**Allen** and **Inoue** perfect video-enhanced light microscopy.
1984	**Agard** and **Sedat** use computer deconvolution to reconstruct Drosophila Polythene nuclei.
1988	Commercial confocal microscopes come into widespread use.
1994	**Chalfie** and collaborators introduce green fluorescent proteins (**GFP**) as a marker in microscopy.

1.2 Fluorescence

Fluorescence can be defined as the emission of light when electrons move from a higher energy state to a state of lower energy [4]. The higher energy and lower energy states are often the first excited state and the ground state respectively. Electrons in stable molecules are in pairs while unstable molecules have unpaired electrons which makes them more reactive. Electrons

have intrinsic angular momentum known as “spin”, and a pair of electrons can be in either of two total spin states depending on the relative symmetry of the spins of the two electrons. If the two spins are in an antisymmetric configuration, then the total spin is equal to zero; otherwise in a symmetric configuration the total spin is 1. The terms singlet and triplet state are also used because there is one combination of electron spin states that is antisymmetric and three combinations that are symmetric as shown in Figure 1.1b [5]. Figure 1-1c [5] is called a Jablonski diagram. It shows the energy transition as electrons move from one energy level to another. When a molecule is excited by a photon of the desired wavelength (λ) the energy absorbed (E) by molecules is given by:

$$E = (\frac{hc}{\lambda}) \qquad 1\text{-}1$$

where h is an inherent property of the molecules and is called the Max Planck constant (value is approximately 6.626×10^{-34} m^2kg/s, c is the velocity of light (value is approximately 3.8×10^{8} m/s^2) and λ is excitation wavelength of light. If this energy is close to the energy difference between the singlet ground states (S_0) and the excited states (S_1) then the electrons are excited very rapidly in the femtoseconds order. Because electrons in these excited states are unstable there is a rapid decay from state S_1 to state S_0 in nanoseconds times scale. This decay is called fluorescence. Molecules can also take another route via intersystem crossing to the excited triplet state (T_1) and then to the ground state (S_0) . The relaxation from T_1 to S_0 is called phosphorescence and occurs at a slower rate of the order of micro to milliseconds. Phosphorescence is very common in molecules that contain heavy metals such as iridium or europium. The decay from T_1 to S_0 is a forbidden transition because they have different spin multiplicity and angular momentum needs to be conserved. The fluorescent emission is at a

longer wavelength compared to the excitation wavelength [6]. As a result of this, there is a difference between the absorption spectrum peak and the emission spectrum peak as shown in the fluorescence spectrum of Green Fluorescent Protein shown in Fig. 1-1d. The peak difference is called the Stokes shift. This shift is important as it allows the emission to be separated from the excitation by a dichroic mirror. Longpass dichroic mirrors transmits wavelengths above a cutoff wavelengths and reflect shorter wavelengths as shown in Fig.1-1d[7].

If a fluorescent molecule is excited at the excitation wavelength continuously to generate several thousands of photons until it becomes permanently dark. In this condition, the molecule is not able to switch between an on state and off state. This phenomenon is called photobleaching and it is a soft limit imposed because of the biochemical properties of the molecules. The fluorescence may be linear or non-linear. In a linear mechanism the intensity of emission linearly depends on that of the excitation light. Otherwise, it is non-linear. The lambert beer law [8]defines describes the reduction in intensity of excitation light (Ie) due to absorption. The intensity of emission (If) , and quantum yield (Q) and intensity of excitation light (Ie) are related mathematically by:

$$If \propto Ie \times Q \times e^{-dcx} \qquad 1\text{-}2$$

Where d, c and x are the extinct coefficients, the concentration, and the optical path length respectively. The parameters determine how much fluorescence we can get from a given excitations. As posited initially, the non-linear mechanism occurs when the excitation and emission are not linear and occurs when a fluorophore absorb too many photons resulting in fluorescence saturation, a phenomenon which is used in saturation excitation microscopy [9].

1.3 Basic Fluorescence Microscope

Fluorescent molecules(fluorophores) can be used to label specific proteins in biological samples, and fluorescent microscopes have become invaluable because they allow specific proteins to be studied. Fluorescence microscopes utilize the fluorescent emission to view region of interest in samples tagged with fluorophores. Research on fluorescent microscopes has provided tools to beat the limit on resolution imposed by diffraction, to image for long times that was initially hampered by soft limits like photobleaching, and to record images rapidly to investigate processes such as the firing of neurons. A basic fluorescent microscope is shown in Figure 1-1e [10]. The sample is mounted on a glass slide and is excited with a laser with wavelength close to the absorption maximum of the fluorophore. The excitation light and the emitted light are separated by a dichroic mirror. The sample is imaged onto a camera by the objective lens and tube lens. An emission filter is placed before the camera that blocks unwanted wavelengths. Basically, the intensity or brightness (which is photon flux per area and time) is directly proportional to the fourth power of the objective numerical aperture but varies inversely to the magnification squared. The numerical aperture of the objective lens is its ability to collect light rays from the sample and the magnification is the ratio of the height of the image to the height of the sample. I discussed more about numerical aperture in chapter two. A bright fluorescent image is obtained with a high numerical aperture objective and a low magnification. As for example an objective lens with magnification of 40x and numerical aperture of 1.4 will produce brighter images than an objective lens with a magnification of 100x and with the same numerical aperture.

1.4 Fluorophores (Fluorescent Probes)

A fluorophore is a molecule which is excited by light and then emits light. Many fluorophores are planar cyclic molecules containing aromatic groups. Common examples of fluorophores are organic fluorophores such as dyes, (as shown in Table 1-2 [11] a,b) , and biological fluorophores such as fluorescent proteins as shown (in Table 1-3a,b,c [11]) . Organic fluorophores are often used in localization microscopy because of high molecular brightness, photon counts and bleaching resistance. However, organic fluorophores can survive fewer switching cycles. Fluorescent probes or fluorophores are used to label or tag regions of interest for visibility when observed in a fluorescent microscope. The precision at which a real biological structure can be localized- "the biological resolution" depends on the labelling efficiency of the probe [12]; on the probe efficiency to bind the target and on the target accessibility. For these reasons, the size of labelling probes is crucial [13]. Upon binding, small probes are closer to the target and enable nice sample penetration in contrast with bigger probes with the same binding efficiency. Antibodies such as IgGs are often employed as probes because they are readily available and have great specificity. However, their relatively large dimensions (approx. 150 kDa in weight and approx. 15 nm in length) can introduce significant artifacts in imaging [14]. This is the reason why smaller affinity probes are preferred to antibodies to stain biological specimens. Recently, VHHs commonly called nanobodies with smaller size (molecular weight of 13 kDa and 3 nm in length) provide excellent monovalent binding with great reduction in artifacts [15]. Nanobodies are now being combined with fluorescent proteins (like rsEGFP) and expressed in cells to highlight the endogenous binders in living cells [16].

Table 1-2a, b [11]. Common organic fluorophores for super-resolution imaging. Notes ps and pa means photo switchable and photoactivable. $\lambda_{ex}\ and\ \lambda_{em}$ are wavelength of excitation, and emission,$brightness = \varepsilon\phi$ where $\varepsilon\ and\ \phi$ are extinction co-efficient and quantum yield respectively.$N\ and\ ND$ are the number of switching cycles and No data reported(parameter not calculated).Phot is the number of photons count per cycle .Organic fluorophores are suitable for super-resolution imaging due to high molecular brightness and photon counts.

a

STED fluorophores	$\lambda_{ex}(nm)$	$\lambda_{em}(nm)$	$\varepsilon(M^{-1}cm^{-1})$	ϕ	$brightness = \varepsilon\phi$
Chromeo 488	488	517	73000	0.38	27740
Chromeo 494	494	628	55000	0.28	15400
Atto 565	563	592	120000	0.9	108000
Atto 647N	644	669	150000	0.5	75000
Fl-Rhodamine	633	653	75000	0.92	69000
Si-Rhodamine	645	662	100000	0.39	39000
AbberiorSTAR635P	635	655	75000	0.92	69000

b

STORM/PALM fluorophores	Notes	$\lambda_{ex}(nm)$	$\lambda_{em}(nm)$	$\varepsilon(M^{-1}cm^{-1})$	ϕ	$brightness = \varepsilon\phi$	N	Phot.
Atto 488(thiol)	ps	501	523	90000	0.8	72000	49	1100
Atto 488	pa	501	523	90000	0.8	72000	~1	$\sim 10^4$
Cy3B(thiol)	ps	559	570	130000	0.67	87100	5	2050
Cy3B	pa	559	570	130000	0.67	87100	~1	$\sim 10^5$
Alexa 647(thiol)	ps	650	665	239000	0.33	78870	26	5200
Cy7(thiol)	ps	747	776	250000	0.28	70000	~3	1000
Alexa 750(TCEP)	ps	749	775	240000	0.12	28800	ND	2800
Si-Rhod. (thiol)	ps	645	662	100000	0.39	39000	ND	630

1.5 Fluorescent Proteins (FPs)

Research into fluorescent proteins started via the discovery of Green Fluorescent Proteins in 1960 when researchers studying the bioluminescent properties of Aequorea victoria jellyfish isolated a blue light emitting protein named aequorin together with another protein that was named Green Fluorescent Protein. GFP derived from Jellyfish has since been genetically modified to produce other variants like blue, yellow, cyan, and red fluorescent proteins. These fluorescent proteins are composed of sequences of amino acids with a light sensitive center called a chromophore. FP can be classified into linear FPs and non-linear FPs. Linear Fluorescent proteins are non-switchable proteins. These proteins are non-photoactivable or photoconvertible. Examples of Linear FPs and properties are stated in Table 1-3a.

Non-linear FPs are those for which the fluorescence is controlled by light of different wavelengths. Photo-controllable FPs are of three types: photoactivatable FPs (PAFPs), photo switchable FPs or photoconvertible (PSFPs or PCFPs) and reversibly photo switchable FPs (rsFPs) . PAFPs can undergo transition from a dark state to an on state but can't be turned back to dark state. A typical example of PAFPs is PAmcherry 1 in Table 1-3c. PSFPs can undergo transition from one state to another but not back and forth between a dark state and an on state. An example is given in figure 1-2 [17] where a Kaede-like FP is transformed from green to red with violet light. On the other hand, rsFPS can be turned repeatedly between a dark state (non-fluorescent state) and an on state (fluorescent state). An example is rsEGFP2 (reversible Enhanced Green Fluorescent Proteins 2) shown in Figure 1-3a, b [10] which is turned on by violet light and turned off by blue light. Another recent rsFPs is red emitting fluorescent proteins as shown in Fig. 1-4 [19]. These proteins can be repeatedly turned on with either blue, violet, or

green light and off with orange light. Although, organic dyes may be superior to FPs in terms of brightness it can be difficult to deliver them to cells and hence require complicated labelling specificity. Examples of non-linear FPs and their properties are given in Table 1-3b, c.

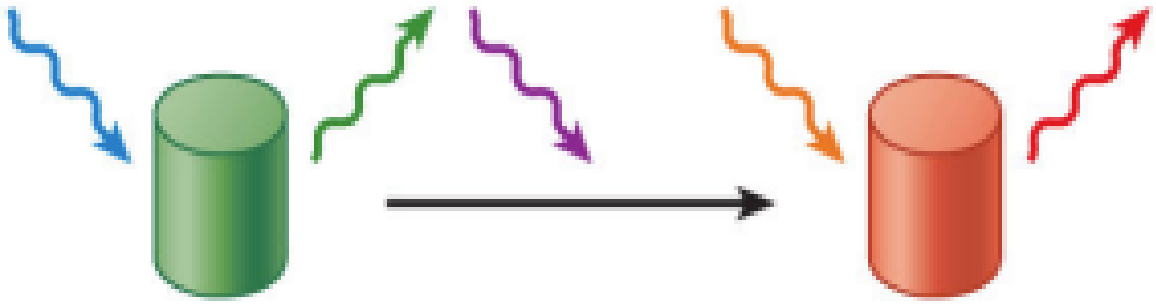

Figure 1-2[17]: A Kaede-like FP transforms irreversibly from green to red with blue and violet light.

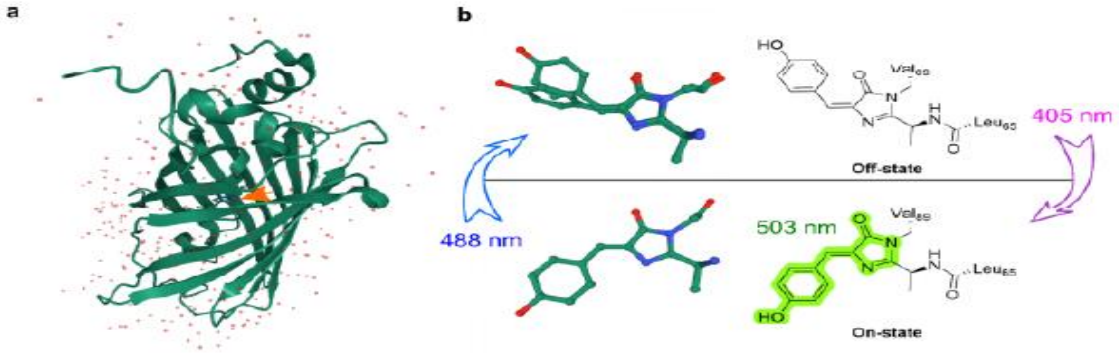

Figure 1-3[10]. a,3-D structure of rsEGFP2 with chromophore (center shown in orange arrow). b, reversible switching of rsEGFP2 shown turned on with 405 nm light and turned off with 488 nm light.

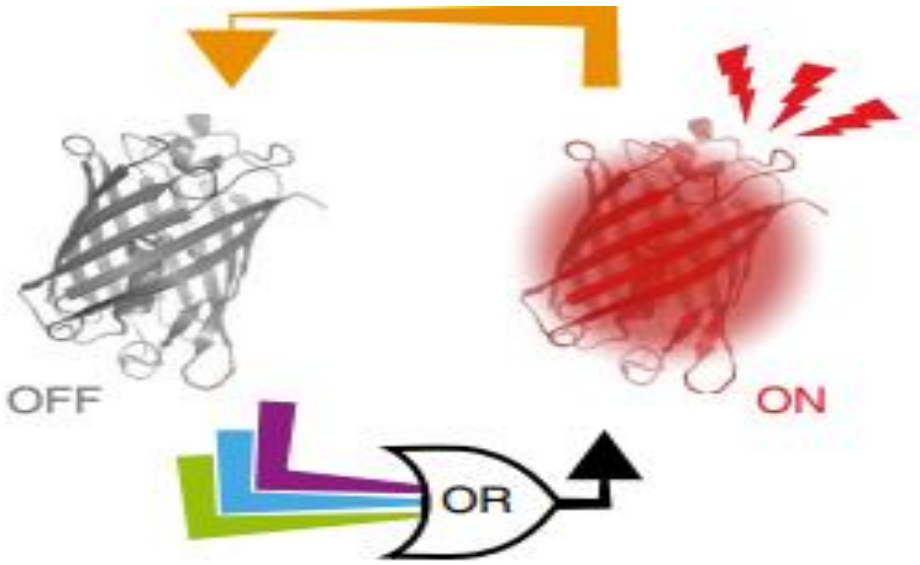

Figure 1-4 [19]. Switching of red fluorescent proteins.Red fluorescent proteins can be repeatedly turned on with either violet, blue, or green light and off with orange light to emit red.

Table 1-3 [10]. Common fluorescent proteins for super-resolution imaging. a,Linear FPs. b, c, Non-Linear FPs. Notes pc, ps, pa, m, t,d,wd means photo convertible, photo switchable and photoactivable,monomeric state,tetrameric state,dimeric state,weak dimeric state.These states are oligomeric state of the fluorescent proteins. λ_{ex} and λ_{em} are wavelength of excitation and emission maximums,$brightness = \varepsilon\phi$ where ε and ϕ are extinction co-efficient and quantum yield respectively.N and ND are the number of switching cycles and No data reported (parameter not calculated) and Phot is the number of photons counts per cycle. Fluorescent proteins are suitable for super-resolution imaging due to large number of switching cycles and photo stability.

a

STED fluorophores	Notes	$\lambda_{ex}(nm)$	$\lambda_{em}(nm)$	$\varepsilon(M^{-1}cm^{-1})$	ϕ	$brightness = \varepsilon\phi$
EGFP	m	490	510	55000	0.6	33000
EYFP	m	514	527	36500	0.63	22995
Citrine	m	516	529	77000	0.76	58520
E2Crimson	t	611	646	126000	0.23	28980
TagRFP657	m	611	657	34000	0.1	3400

b

RESOLFT/SIM fluorophores	Notes	$\lambda_{ex}(nm)$	$\lambda_{em}(nm)$	$\varepsilon(M^{-1}cm^{-1})$	ϕ	$brightness = \varepsilon\phi$	N
Dronpa	m, ps	503	518	95000	0.85	80750	60-70
rsEGFP	m, ps	493	510	47000	0.36	16920	>1100
rsEGFP 2	m, ps	478	503	61300	0.3	18390	>2000
Dreiklang	m, ps	511	529	83000	0.41	34030	>160
rsCherryRev1.4	d, ps	572	609	ND	ND	ND	>1000

c

STORM/PALM fluorophores	Notes	$\lambda_{ex}(nm)$	$\lambda_{em}(nm)$	$\varepsilon(M^{-1}cm^{-1})$	ϕ	$brightness = \varepsilon\phi$	Phot.
PAmcherry 1	m, pa	564	595	18000	0.46	8280	~725
Dronpa	m, ps	503	518	95000	0.85	80750	120
Dreiklang	m, ps	511	529	83000	0.41	34030	400-700
MEos2	wd, pc	569	581	41000	0.55	22,550	~1000
MEos3.2	m, pc	572	580	32200	0.55	17710	~1000
mMaple	wd, pc	566	583	30000	0.56	16,800	~1000
mMaple2	m, pc	566	583	ND	ND	ND	~800

1.6 Generation of rsEGFP 2 (reversible Enhanced Green Fluorescent Proteins 2)

Reversible Enhanced Green Fluorescent Protein 2 is generated by replacing the threonine with alanine in the 65th position of the amino acid sequence in the chromophore as shown in the figure 1-5 below [18]. This mutation results in the RSFP having a fast-switching characteristic and a negative switching behavior. By negative switching (as shown in figure 1-3b) we mean that rsEGFP2 can switch from the on state to the off state with blue light (wavelength ~480 nm) which is also used to read out the fluorescence (~510 nm) and then switched from the off state back to the on state by violet light (at wavelength ~405 nm) . The 3-D structure of rsEGFP2 is also shown in figure 1-3a with the light controlling center (chromophore) shown with orange arrow.

```
                1                                                   47
EGFP            MVSKGEELFTGVVPILVELDGDVNGHKFSVSGEGEGDATYGKLTLKFI
rsEGFP          MVSKGEELFTGVVPILVELDGDVNGHKFSVSGEGEGDATYGKLTLKFI
rsEGFP2         MVSKGEELFTGVVPILVELDGDVNGHKFSVSGEGEGDATYGKLTLKFI
               48                  65  69                       95
EGFP            CTTGKLPVPWPTLVTTLTYGVQCFSRYPDHMKQHDFFKSAMPEGYVQE
rsEGFP          CTTGKLPVPWPTLVTTLTYGVLCFSRYPDHMKQHDFFKSAMPEGYVQE
rsEGFP2         CTTGKLPVPWPTLVTTLAYGVLCFSRYPDHMKQHDFFKSAMPEGYVQE
```

Figure 1-5[18]. Amino Acid sequence of chromophore of EGFP, rsEGFP and rsEFGP2. At the 65th position threonine is replaced by alanine as shown.

1.7 Need for non-linear Fluorescent Proteins

Non-linear fluorescent proteins such as rsEGFP 2, rsEGFP, Dronpa and asFP595 are needed for super resolution microscopy because they provide improved resolution image at sub diffraction levels, has longer switch cycles and provide faster image acquisition. As for example, asFP595 expressed in the bacteria Escherichia coli was used to achieve 50 nm resolution [19]. U2OS cells expressing rsfusionRed1 showed fast off-switching kinetics of about 58.3 ms and a sub-diffraction wavelength of 62 nm was achieved [20]. Dronpa has been used to achieve less than 50 nm resolution of various in vitro or cellular structures[21]. Dreiklang and rsEGFP has been used to photo switch more than 1000 cycles and to achieve less than 40nm resolution in fixed cells[22].In living cells rsEGFP2 and rsCherryRev 1.4 have been used in one and two-color RESOLFT imaging to achieve resolution less than 50 nm [18] and rsEGFP2 was used to image vimentin at faster speed of 0.24 s [18].Molecular brightness of rsEGFP2 is often lower than that of linear fluorescent proteins as seen in comparison of the brightness of rsEGFP2 to linear FP's in table 1-3a and b. However, the genetic mutations involved in replacing threonine with alanine in rsEGFP to obtain rsEGFP2 makes it a faster switching protein and with superior properties. As for example, the single molecule brightness of rsEFP2 is approx. 1.08 times that of rsEGFP as shown in Table 1-4 [18], quick maturation (chromophore maturation halftime of rsEGFP2 is 9 times faster than rsEGFP at 37 degree Celsius) [18], high switch fatigue resistance (fluorescence was halved not before approx. 1,100 and 2,100 for rsEGFP and rsEGFP2 respectively) as shown in Fig. 1-6) [18],photostable and faster image recording(at low light intensity of 5.5 KW/cm^2, the off switching speed of rsEGFP2 was 6.5 times faster than off switching of rsEGFP and 25-

250 faster recordings in living cells were obtained with RESOLFT(Reversible Saturable Optical Fluorescence Transitions)) [18].Table 1-4 shows the properties of rsEGFP2 in comparison to EGFP and rsEGFP2.Due to higher switch fatigue resistance more switching cycles can be obtained and there is more frequency information and consequently high resolution in the image. A resolution of less than 50 nm was obtained when cells expressing Keratin19-rsEGFP2 were imaged using reversible saturable optical fluorescence transitions (RESOLFT) microscopy methods [23].

Table 1-4 [18]. Comparison of EGFP, rsEGFP and rsEGFP2. rsEGFP2 shows faster chromophore maturation and better switch fatigue resistance as it can survive more switching cycles. Brightness of rsEGFP 2 is also higher than that of rsEGFP.

Fluorescent proteins	$\lambda_{ex}(nm)$	$\lambda_{em}(nm)$	$\varepsilon(M^{-1}cm^{-1}$	ϕ	$\varepsilon\phi$	Number of switching cycles to bleach to 50%	Chromophore maturation halftime at 37^0C(min)
EGFP	489	509	53000	0.6	31800	N. A	25
rsEGFP	493	510	47000	0.36	16920	~1100	~180
RsEGFP 2	478	503	61300	0.3	18390	~2100	~20

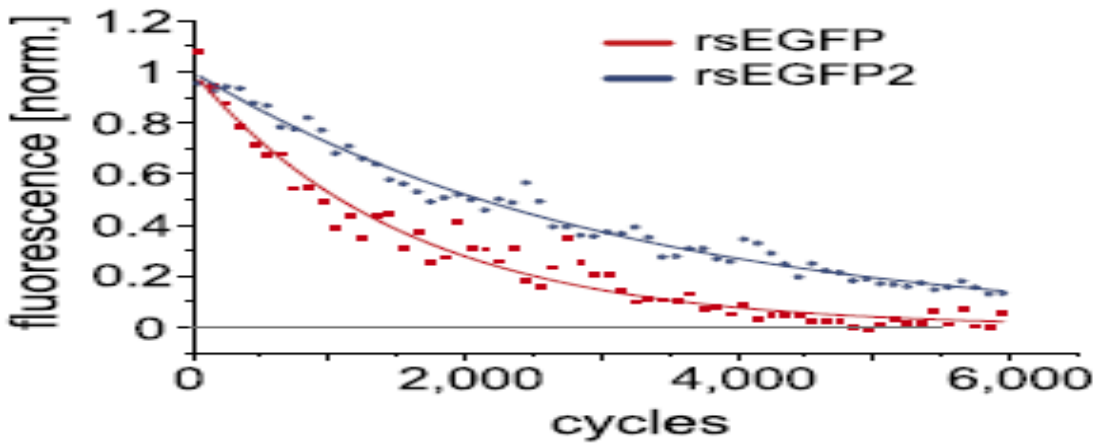

Figure 1-6 [18]. Switch cycles of rsEGFP (red) and rsEGFP2 (blue) . At normalized fluorescence of 0.5 rsEGFP (red) and rsEGFP 2 (blue) has ~1100 and ~2100 switching cycles indicating

higher switch fatigue resistance in rsEGFP 2. Switching was performed on living ptk2 cells expressing Vimentin using RESOLFT by alternate irradiation with 405 nm (2 kW/cm²) and 491 nm (5.7 kW/cm²) light.

1.8 Super Resolution Imaging Techniques

Two key events in 1994 in the field of microscopy led to breakthroughs in chemistry and biology. One involved the discovery of genetically encoded green fluorescent proteins [24]and the other is a way to bypass the hard limit imposed by the diffraction of light in imaging. These methods used to break the limit imposed by the wavelength of light due to diffraction are called super resolution techniques [19]. This limit is half the wavelength of light in the visible spectrum range which is about 200 nm. These two discoveries revolutionized the field of fluorescence microscopy and led to an award of a Nobel prize in chemistry in 2008 and 2014. Despite, all the breakthroughs, super resolution techniques still have some technical limitations because sample preparation can be challenging, and photo damage can be a problem. The main super resolution techniques often used are the STED (Stimulated Emission Depletion Microscopy) , SIM (Structured Illumination Microscopy) and SMLM (Single Molecule Localization Microscopy such as STORM and PALM) . Below I explained in brevity how the processes work.

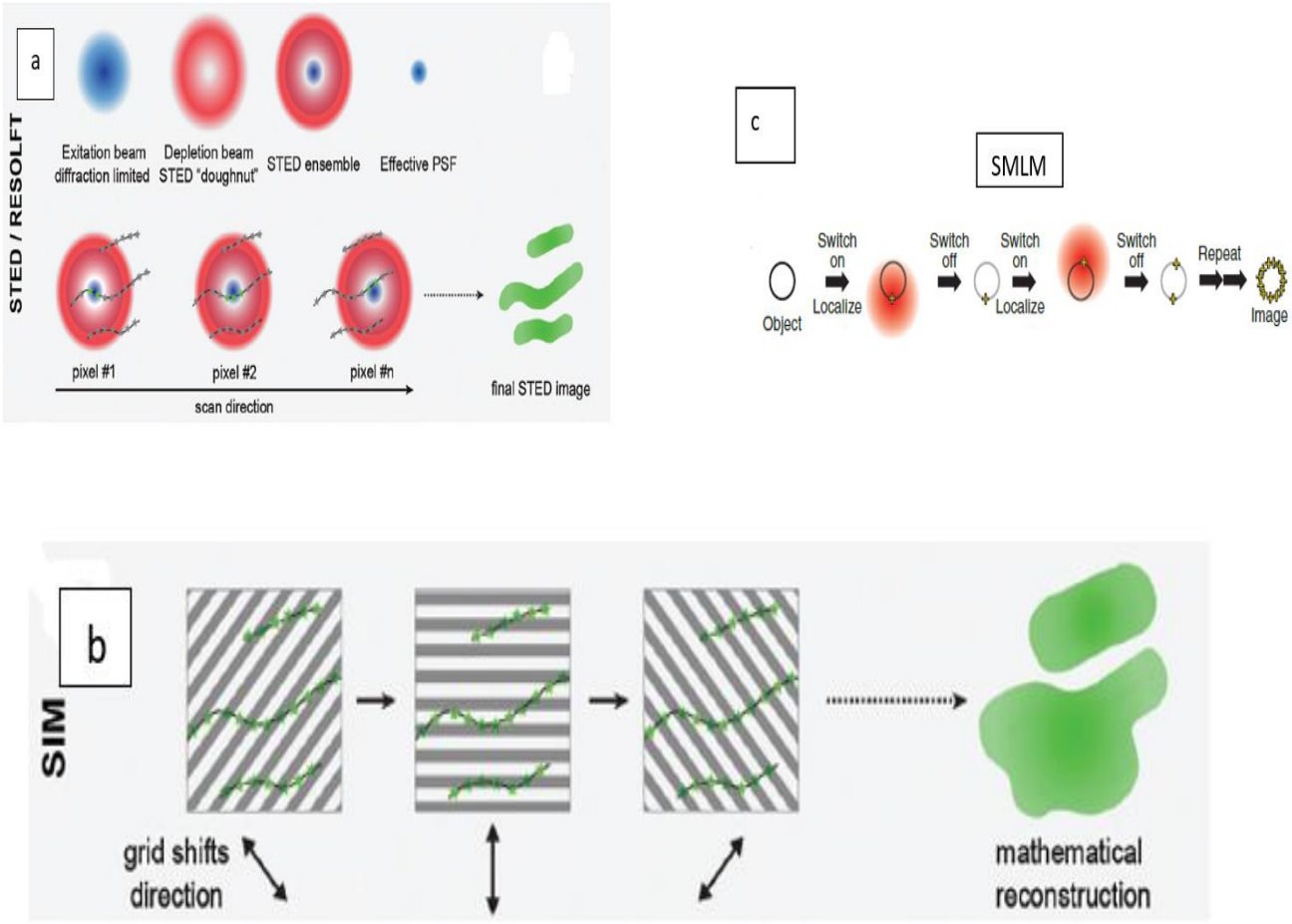

Figure 1-7. a, Basic of STED.violet line with arrows read out pixels (blue is excitation beam and red circle is depletion beam [25]. b,SIM uses illumination patterns (grey) to modulate sample(blue) [26].c,SMLM turns a subset of molecules ON (yellow center) using red light and locate their center. By moving the laser in different positions different points are localized to obtain a high resolved ring structure [27].

1.9 Simulated Emission Depletion Microscopy (STED)

Images are assembled in STED on a pixel by pixel scan basis with a laser (violet) and a pinhole removes out of focus light in the optical path as shown in Fig.1-7a [25].Lateral resolution improvement depends on simultaneous illumination of the sample with a second long-wavelength (red) laser which selectively switch off a population of the energized

flurophores.This laser is called the depletion beam and is doughnut shape with a low intensity at the center and highest at the periphery of the beam. This design enables more stimulated emission ("switch off") around the center and only emitting fluorophores at the center provide strong imaging depths. As a result, a highly resolved imaged (determined by the small size of the central region not switched off by the depletion beam) is obtained. To achieve this high resolution a powerful depletion laser is often needed but this has photobleaching effect to the sample. STED is well documented to achieve lateral and axial resolution of as low as 20 nm.

1.10 Structured Illumination Microscopy (SIM)

As shown in Fig. 1-7b [26], in SIM the sample is excited by an illumination pattern (grey in the figure). This results in a moire fringe pattern which shifts higher frequency sample information into the OTF support of the microscope. The high frequency information provides higher resolution. To achieve a well resolved final image, the illumination pattern needs to be rotated through different angles to obtain an isotropic space. A two-fold lateral resolution is achieved in 2D linear SIM image and up to a 5-fold increase can be achieved in non-linear SIM techniques such as saturated structured illumination microscopy [9].

1.11 SMLM (Single Molecule Localization Microscopy)

SMLM, as shown in Fig.1-7c [27], localizes individual fluorescent molecules using their intensity profiles (Gaussian profiles are commonly used where the apex of the Gaussian coincides with the center of the fluorophore). The key principle in SMLM is to turn on (using red laser) or off (using blue laser) a subgroup of sparse fluorescent molecules in different imaging

cycles [27]. The accuracy of SMLM depends on having only a few emitters per image cycle whose centers (shown yellow) can be accurately localized. The resolution depends on the number of photons collected from each emitter and the suitability of the dyes used. Thousands of images are needed to localize the fluorophores to obtain a highly resolved image. SMLM has achieved lateral and axial resolution as low as 10nm and 20nm respectively.

1.12 This Work

Clearly, there have been lots of breakthroughs in fluorescence microscopy but in this thesis, I will characterize reversibly photo switchable Enhanced Green Fluorescent Proteins 2 (rsEGFP 2) to evaluate its suitability for Nonlinear Structured Illumination Microscopy (NSIM). I will characterize the protein by measuring the switching fatigue, the activation and depletion time constants, the variation of peak fluorescence and time constant with exposure time and the variation of the ratio of background to peak fluorescence with exposure time. These parameters are key because they influence the amount of fluorescence that is detected by the sensor of the camera and the level of resolution achieved. With a low switch fatigue more image frames can be capture by the camera and this will improve resolution. Also, the decay times determine waiting times to achieve a certain amount of non-linearity. Hence, it also influences the image resolution. The peak fluorescence and time constant provide information on how the fluorescence also changes with exposure time increase since they influence the fluorescence. The ratio of background to peak fluorescence also provides how much of the fluorescence constitute

background. Ideally, this ratio should decrease with increase in exposure time so that the fraction of background fluorescence is small.

Most of the work done in characterizing proteins has been on localization microscopy and RESOLFT because the former involves counting of emitters (fluorophores) that are turned on and the latter uses low light levels. The accuracy of localization microscopy depends on the stochasticity, or the probability of emitters turned on in a switching event. As for example Travis Gould et al. [28]characterized Drendra2 at frame rates of approx. 30 Hz, laser power of 104 Wcm-2 of 556 nm read out and continuous 405 nm activation(approx.0.6-6 Wcm-2) in FPALM (Fluorescence Photoactivation Localization Microscopy) . Daria Schcherbakova et al. [17] characterized rsFP in nanostructures in a process called RESOLFT (Reversible Saturable Optical Fluorescence Transition) in living cells. Graham Dempsey et al. [26] provide a comprehensive characterization of dyes used for localization based super resolution imaging. .Micheal Hofmann et al. [23] characterized Dronpa in STED microscopy with reported resolution of 30nm. Tim Grotjohan et.al [18] characterized rsEGFP and rsEGFP 2 expressed in vimentin cells.

1.13 Outline of the thesis

In this introduction chapter I provide a brief history of microscopy, description of the basic fluorescence microscope, fluorescence spectrum and the Jablonski diagram. I also gave a brief review of the common fluorescence microscopy techniques and fluorescent markers/probes. In chapter 2, I provide fundamentals of optical setups (resolution, numerical aperture and Image formation and point spread function). In addition, a detailed analysis of 2D and 3D SIM is provided.

In chapter 3, a detailed description of non-linear SIM is presented with specific reference to rsEGFP2.

In Chapter 4, I explain switch fatigue and decay constants are presented. A description of the experimental set up and results of the experiments are explained.

In chapter 5, Conclusions of the work and recommendations for future work are presented.

Chapter Two

Fundamental of Optical Systems

2.1 Spatial Resolution

Image formation in microscopy is linear. The imaging system obeys the super-position principle. The image is scaled by the same factor as the object, and the image is the total sum of the contributions of the image from different points on the object. As a result, in considering image formation, it is safe to analyze points on the object. The spatial resolution of a microscope is the smallest possible separation of two points for which the two points can be distinguished. As shown in Fig. 2-1 [10], a microscope with a higher resolution can distinguish closer points compared with a lower resolution. This resolution is limited by the physical laws of diffraction, and it is approximately half the wavelength of light. For visible light, laterally, this is about 250nm for traditional widefield microscopes. The spatial resolution can also be described in the equivalent space of reciprocal frequencies, the Fourier domain. As shown in Fig. 2-1, the Fourier domain is the Fourier transform of the spatial domain to obtain a Fourier spectrum. The Fourier spectrum is a plot of the Fourier coefficients obtained from the Fourier transform against the frequency. A large area in the frequency space bounded by this spectrum means a higher resolution. This also follows from the bottom row of Fig.2-1 that images with high spatial resolution have a circle with higher radius. This means the support for high frequency information is high for high spatial resolution.

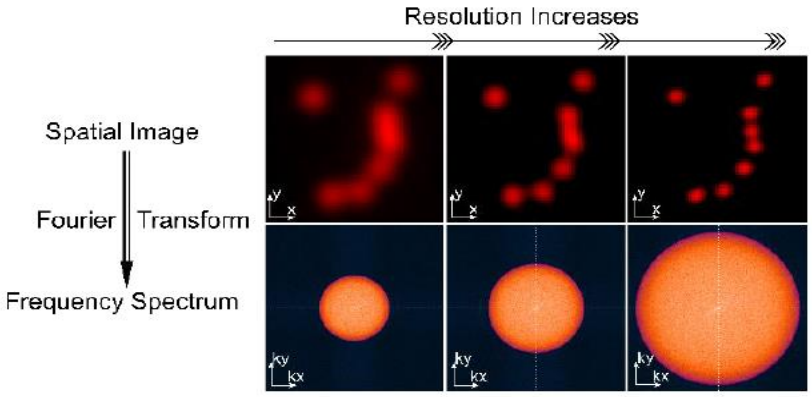

Figure 2-1 [10]. Spatial and frequency domain.

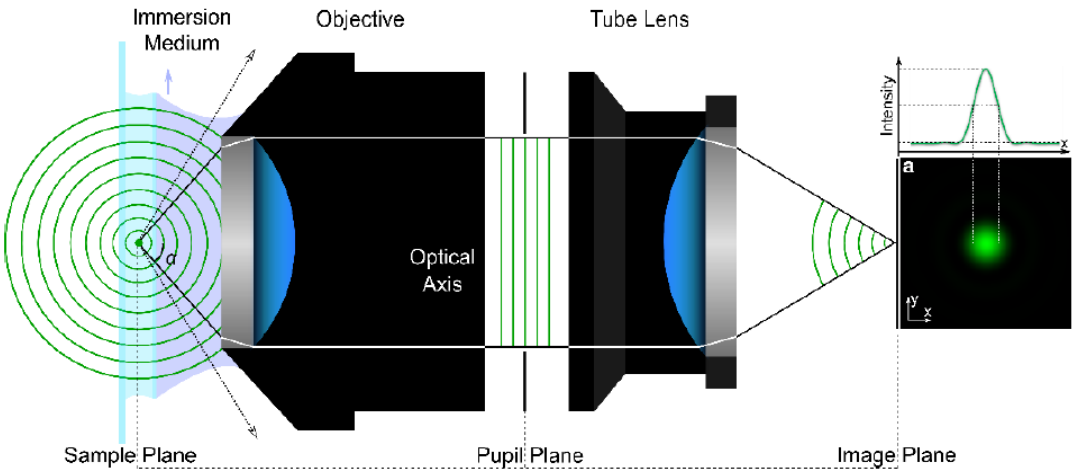

Figure 2-2 [10]. Image formation in an optical system. Diameter of green blurred spot is the spatial resolution. The intensity distribution (green plot) is the Point Spread Function.

Lights from different points on the objects leaves as spherical wavefronts. As a result, only a cone of light is collected by the objective lens as shown in Fig. 2-2[10]. The angular half-width times the refractive index is the numerical aperture (NA). If the angular half-width of the objective is denoted by $\propto$ then the numerical aperture (NA) is given by:

$$NA = nsin \propto \qquad 2\text{-}1$$

Where n is the refractive index of the medium between the sample and the objective lens. This can be water, air, or oil. By convention, $\propto$ is defined to be half of the full aperture angle of the objective lens and angles beyond $\propto$ means that the light will not be captured by the objective. The higher the refractive index (such as using oil with a value of 1.51) the greater the NA. However, oil-based lens may be expensive. The object is mostly at the front focal plane of the objective so that the lights will emerge parallel(collimated) to the optical axis and pass through the pupil plane at the back focal plane of the objective. For a coherent light source (point source)

the PSF is given by the Fourier transform of the pupil function ($P(x,y)$). Mathematically, this is given by:

PSF=$\iint_{-\infty}^{\infty} P(x,y)e^{-j2\pi(xu+yv)}dxdy$ 2-2

Equation 2-2 is a 2D Fourier from the (x, y) co-ordinates in the spatial domain to the (u, v) co-ordinate in the frequency domain.

The complex amplitude at the pupil plane is given by:

$Uo(u,v) = \iint_{-\infty}^{\infty} O(\xi,\mu).PSF\ d\xi d\mu$ 2-3

where $O(\xi,\mu)$ is the object and ξ μ are the co-ordinates of the object's location in space. The pupil function describes how the amplitude and phase of a spherical wave front is changing as it propagates in an optical set up. Mathematically, the pupil function can be given by:

$P(u,v) = B(u,v)e^{j\emptyset(u,v)}$ 2-4

Where $\emptyset(u,v)$ is the phase change and $B(u,v)$ is the amplitudes at the pupil plane.

In ideal cases, the objects are not point sources like a laser light and it is often difficult to get an interference pattern from a set of those sources. A typical example is a LED light which is incoherent. In this system, the autocorrelation of the pupil function is an aperture of finite size. This virtual aperture is called the OTF (Optical Transfer Function). The OTF provides the extent to which frequencies from the object are transferred to the image. Mathematically, the OTF is given by:

$OTF(kx,ky) = \iint_{-\infty}^{+\infty} P*(u,v).P(u+kx,v+ky)dudv$ 2-5

Where the term $P*(u,v)$ is the same as the Fourier transform of $P(-u,-v)$. The magnitude of the OTF is called the MTF (Modulated Transfer Function) and it is used to assess the quality of the optical system. Ideally, the image of a point object should give a sharp point image. However, due to the finite size of the OTF support the image is not sharp but a blurred one. The intensity distribution of this blurred image is called the point spread function of the microscope and it is often used to characterize the performance of a microscope in respect of the imaging quality. It is also regarded as the impulse response of the microscope. Which is the response when the object is a Dirac Delta function. The PSF of a point object is the full width at maximum (FWHM) of the intensity distribution. In a traditional wide field microscope, the spatial resolution along the lateral(x-y) and axial(z) directions are given by:

$$Rxy = \lambda/2NA \qquad 2\text{-}6$$

$$Rz = 2\lambda/NA^2 \qquad 2\text{-}7$$

Obviously, the PSF is a key parameter because it determines the resolution of the microscope and an inherent property of the optical design. Regardless of the properties of coherence, the Image is the convolution of the object with the PSF in the spatial domain and the multiplication of their respective Fourier transform in the space of reciprocal frequencies. Mathematically, we can write:

$$Image(\boldsymbol{r}) = Object(\boldsymbol{r}) \otimes PSF(\boldsymbol{r}) \qquad 2\text{-}8$$

$$Image(\boldsymbol{k}) = Object(\boldsymbol{k}).OTF(\boldsymbol{k}) \qquad 2\text{-}9$$

2.2 Theory of 2-D Linear Structured Illumination Microscopy (SIM)

In Linear 2-D Structured Illumination Microscopy the Emission intensity varies linearly with the Illumination intensity. Also, the illumination has a sinusoidal intensity pattern that results in a frequency aliasing effect where higher spatial frequencies in the sample are imaged at lower spatial frequencies resolvable by the microscope. The illumination pattern is generated in such a way that it modulates frequencies of the object and as a result shift higher frequency outside of the OTF support of the microscope to within it (Figure 2-3 [10]) . These higher frequencies (Figure 2-4 [10]) are encoded within the low frequencies and will be separated computationally and then restored to appropriate points in reciprocal space. The sample ($O(r)$) in this case is a distribution of markers and the Illumination pattern($I(r)$)for simplicity is often sinusoidal and of the form given by:

$$I(r) = 1 + \cos(2\pi \boldsymbol{k}_0 \boldsymbol{r} + \boldsymbol{\phi}) \qquad 2\text{-}10$$

Where $\boldsymbol{k}_0$ and $\boldsymbol{r}$ are the wave vector and the spatial co-ordinates vectors in 2-D and $\boldsymbol{\phi}$ is the phase of the pattern and $\boldsymbol{k}_0$ determines its orientation.

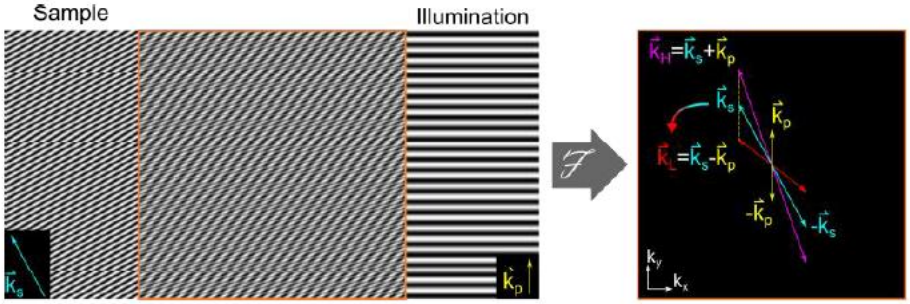

Figure 2-3 [10]. Pictorial illustration of SIM. In the middle rectangle region, the illumination is superimposed with the sample resulting in moiré fringes. k_s and k_p are respectively spatial frequencies of the sample and patterned light (k_0) is used in the mathematical analysis. The right is the Fourier transform and it shows the high frequency information k_H and k_s which is encoded within k_L. They are separated using algorithms.

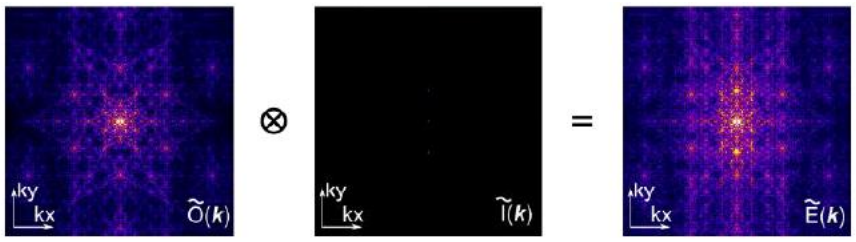

Figure 2-4[10]. Pictorial effects of SIM. The convolution of the object and the pattern in the Fourier space results in more high frequency information as can be seen from two dots (above and below the bright center dots).

The Illumination pattern has a Fourier transform given by:

$$I(\boldsymbol{k}) = \delta(\boldsymbol{k}) + 0.5\delta(\boldsymbol{k} + \boldsymbol{k}_0)e^{j\phi} + 0.5\delta(\boldsymbol{k} - \boldsymbol{k}_0)e^{-j\phi} \quad 2\text{-}11$$

The fluorescent emission is proportional to the illumination for every location within the sample.

Hence, it is given by:

$$E(\boldsymbol{r}) = O(\boldsymbol{r}).I(\boldsymbol{r}) \quad 2\text{-}12$$

In the space of spatial frequencies equation 2-11 is given by:

$$E(\boldsymbol{k}) = O(\boldsymbol{k}) \otimes I(\boldsymbol{k}) \quad 2\text{-}13$$

Where I have taken the Fourier transform of the LHS and the RHS of equation 2-12 and the multiplication become a convolution in the frequency domain. If we substitute for $I(\boldsymbol{k})$ in 2-13 and we invoke the distributive property (2-14) and convolution with delta property of Fourier transform (2-14) we obtain 2-15.

$$(a + b) \otimes c = (a \otimes c) + (b \otimes c) \quad 2\text{-}14$$

$$a(k) \otimes \delta(k - k_0) = a(k - k_0) \quad 2\text{-}15$$

$$E(k) = O(k) + 0.5O(\boldsymbol{k} + \boldsymbol{k}_0)e^{j\phi} + 0.5O(\boldsymbol{k} - \boldsymbol{k}_0)e^{-j\phi} \quad 2\text{-}16$$

The emission spectrum consists of three components. The Fourier transform of the original sample with amplitude of 1. A delta function at $\boldsymbol{k}_0$ with an amplitude of 0.5 and another at $-\boldsymbol{k}_0$ with an amplitude of 0.5. These two delta functions are shifted copies of the original sample with lower amplitude but contains higher frequency information which are encoded within the sample. By repeating this procedure with $\boldsymbol{k}_0$ pointed in other directions and with different ϕ we can retrieve and restore essentially all the information from a circle with twice the radius of the normally observable region. Hence, a 2-D SIM produces a reconstructed image with twice the normal, diffracted-limited resolution which is about 100nm [29]. This limit is set by the fact that the pattern phase ($\boldsymbol{k}_0$) depends on the wavelength of the excitation light.

The image sensor of the camera captures image ($D(r)$) which is a convolution of Emission ($E(r)$) and the PSF. Mathematically, we can write:

$$D(\boldsymbol{r}) = E(\boldsymbol{r}) \otimes PSF \quad 2\text{-}17$$

In reciprocal frequency space, this becomes:

$$D(\boldsymbol{k}) = E(\boldsymbol{k}).H(\boldsymbol{k}) \quad 2\text{-}18$$

Where $H(\boldsymbol{k})$ is the optical transfer function (OTF) of the diffraction limited image. Putting $E(\boldsymbol{k})$ in 2-15 into 2-17 we have:

$$D(\boldsymbol{k}) = O(\boldsymbol{k}).H(\boldsymbol{k}) + 0.5O(\boldsymbol{k} + \boldsymbol{k}_0)e^{j\phi}.H(\boldsymbol{k}) + 0.5O(\boldsymbol{k} - \boldsymbol{k}_0)e^{-j\phi}H(\boldsymbol{k}) \quad 2\text{-}19$$

2.3 2-D Linear SIM Image Reconstruction

The image captured by the camera ($D(\boldsymbol{k})$ in equation 2-19 consist of three components the normal diffraction limited image ($O(\boldsymbol{k}).H(\boldsymbol{k})$) and two shifted copies: $0.5O(\boldsymbol{k}+\boldsymbol{k}_0)e^{j\phi}.H(\boldsymbol{k})\ and\ \ 0.5O(\boldsymbol{k}-\boldsymbol{k}_0)e^{-j\phi}H(\boldsymbol{k})$ which contains high frequency information shifted by the Illumination pattern($\boldsymbol{k}_0$)**.**To cover an isotropic space, three pattern phase ($\boldsymbol{k}_0$) and phase(ϕ) in steps of 60degrees are needed. Hence, resulting in a total of 9 images. Mathematically, we can write $D(\boldsymbol{k})$ as:

$$D(\boldsymbol{k})=D_O(\boldsymbol{k})+ D_{+1}(\boldsymbol{k})+D_{-1}(\boldsymbol{k}) \quad \text{2-20}$$

Where:

$$D_O(\boldsymbol{k})= O(\boldsymbol{k}).H(\boldsymbol{k}) \quad \text{2-21}$$

$$D_{+1}(\boldsymbol{k})= 0.5O(\boldsymbol{k}-\boldsymbol{k}_0)e^{-j\phi}H(\boldsymbol{k}) \quad \text{2-22}$$

$$D_{-1}(\boldsymbol{k})= 0.5O(\boldsymbol{k}+\boldsymbol{k}_0)e^{j\phi}.H(\boldsymbol{k}) \quad \text{2-23}$$

As before equation 2-22 and 2-23 are shifted copies of the original object. To restore the original object the frequencies are shifted to their appropriate points in reciprocal space. Hence, equation 2-22 and 2-23 becomes:

$D_{+1}(\boldsymbol{k}+\boldsymbol{k}_0)= 0.5O(\boldsymbol{k})e^{-j\phi}H(\boldsymbol{k}+\boldsymbol{k}_0)$ 2-24

$D_{-1}(\boldsymbol{k}-\boldsymbol{k}_0)= 0.5O(\boldsymbol{k})e^{j\phi}H(\boldsymbol{k}-\boldsymbol{k}_0)$ 2-25

The final reconstructed image is given by:

$S(\boldsymbol{k})=(D_O(\boldsymbol{k})H^*(\boldsymbol{k})+D_{+1}(\boldsymbol{k}+\boldsymbol{k}_0)H^*(\boldsymbol{k}+\boldsymbol{k}_0) + D_{-1}(\boldsymbol{k}-\boldsymbol{k}_0)H^*(\boldsymbol{k}-\boldsymbol{k}_0)) /(\text{abs}(H(\boldsymbol{k})))^2 +$

$(\text{abs}(H(\boldsymbol{k}+\boldsymbol{k}_0)))^2 + (\text{abs}(H(\boldsymbol{k}-\boldsymbol{k}_0)))^2+w^2$) 2-26

Where in 2-26 w is the wiener filter parameter and the symbol * is the complex conjugate and abs represent the absolute value or modulus.

2.3 Theory of 3-D Linear Structured Illumination Microscopy

A 3D illumination pattern can be generated by interference of three coherence beam of light and with different magnitudes for k_z. Consequently, the 3D illumination pattern generated is given by:

$I(\boldsymbol{r}) = \Sigma_j B_j(\boldsymbol{r_z}).C_j(\boldsymbol{r_{xy}})$ 2-27

Where $C_j(\boldsymbol{r_{xy}}) = d_j e^{i(2\Pi k_j r_{xy}+\phi_j)}$ and $B_j(\boldsymbol{r_z})$ are the x-y components of the patterned light and z components respectively.

As before, the Emission ($E(\boldsymbol{r})$ is given by:

$$E(\boldsymbol{r}) = \Sigma_j O(\boldsymbol{r}).I(\boldsymbol{r}) \quad \text{2-28}$$

Also, as before image captured by the camera in spatial domain is given by:

$$D(\boldsymbol{r}) = E(\boldsymbol{r}) \otimes PSF \quad \text{2-29}$$

Putting $E(r)$ in 2-20 into 2-21, we have:

$$D(\boldsymbol{r}) = \Sigma_j O(\boldsymbol{r}).B_j(\boldsymbol{r_z}).C_j(\boldsymbol{r_{xy}}) \otimes PSF \quad \text{2-30}$$

For simplicity, we can assume that the z – components ($B_j(r_z)$ is the optical axis of the objective and the illumination pattern is fixed relative to its focal lens then the convolution of ($B_j(r_z)$ and $O(r)$ with the PSF is effective OTF ($H(k)$. And the image in the space of reciprocal frequencies is described as:

$$D(\boldsymbol{k}) = \Sigma_j H(\boldsymbol{k}).d_j\, e^{i(\phi_j)}.O(\boldsymbol{k} - \boldsymbol{k_j}) \quad \text{2-31}$$

Equation 2-23 shows that for every component there is a phase shift term (ϕ_j) and a spatial frequency shift term (k_j) modulated by the OTF ($H(\boldsymbol{k})$).

The generation of the 3-D patterned light and filling the missing cones is as shown in Figure 2-5[10] below.

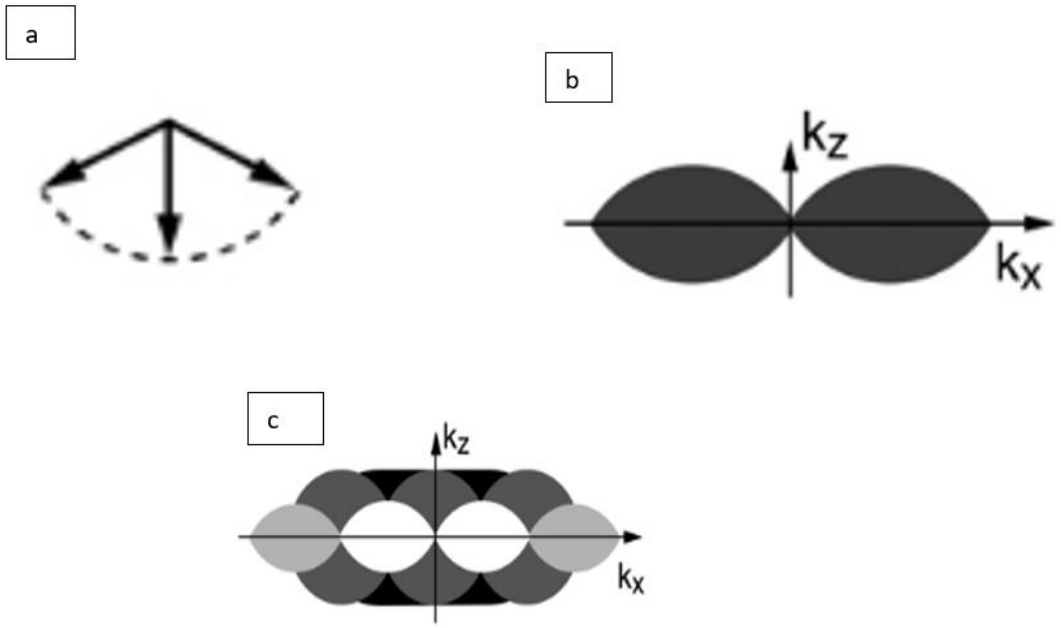

Figure 2-5 [30]. Pictorial illustration of 3D SIM. a, Three beams interference. b,Diffraction limited OTF support showing missing cones.c, The OTF support after interference and frequency mixing with the diffraction limited support showing filled cones laterally and axially.

3-D Linear Structured Illumination Microscopy Image Reconstruction

The patterned light is obtained via interference of beams with wavevectors ($k_{-1}, k_{+1} and\ k_{0,}$) along the optical (z) axis. The original OTF support of the original object is shown adjacent and the new OTF support is shown(b) indicating the missing cones has been filled with copies(red lobes).Since, the Fourier transform is linear and symmetrical the pair of lobes can be regarded as same and it therefore contains five spatial components ($0, \pm k_{xy}\ and \pm 2k_{xy}$) and three axial components ($0, \pm k_z$) . The components ($\pm k_{xy}, \pm k_z$) are the 1st order terms and the components

$(\pm 2k_{xy}, 0)$ are the zero order terms. The 1st order terms are the shifted copies, and they constitute high frequency information while the zero order terms are normal diffraction limited terms. The lateral (k_{xy}) and axial resolution (k_z) are $\frac{NA}{\lambda}$ and $NA^2/2\lambda$ at their peak. The sinusoidal patterns are rotated in three angles with steps of 60 degrees and five phases with steps of $2\pi/5$ to cover an isotropic region with a resolution twice the diffraction limited at best in both axial and lateral directions. Like 2D, 3D image captured by the camera is given by:

$$D(\boldsymbol{k})=D_O(\boldsymbol{k})+ D_{+1}(\boldsymbol{k})+D_{-1}(\boldsymbol{k}) +D_{+2}(\boldsymbol{k}) + D_{-2}(\boldsymbol{k}) \quad 2\text{-}32$$

Where:

$$D_O(\boldsymbol{k}) = O(\boldsymbol{k}).H(\boldsymbol{k}) \quad 2\text{-}33$$

$$D_{+1}(\boldsymbol{k}+\boldsymbol{k}_0)= 0.5O(\boldsymbol{k})e^{-j\phi}H(\boldsymbol{k}+\boldsymbol{k}_0) \quad 2\text{-}34$$

$$D_{-1}(\boldsymbol{k}-\boldsymbol{k}_0)= 0.5O(\boldsymbol{k})e^{j\phi}H(\boldsymbol{k}-\boldsymbol{k}_0) \quad 2\text{-}35$$

$$D_{+2}(\boldsymbol{k}+\boldsymbol{2k}_0)= 0.5O(\boldsymbol{k})e^{j\phi}H(\boldsymbol{k}+\boldsymbol{2k}_0) \quad 2\text{-}36$$

$$D_{-2}(\boldsymbol{k}-\boldsymbol{k}_0)= 0.5O(\boldsymbol{k})e^{j\phi}H(\boldsymbol{k}-\boldsymbol{2k}_0) \quad 2\text{-}36$$

The final reconstructed image is given by:

$$S(\boldsymbol{k})=(\ D_O(\boldsymbol{k})H^*(\boldsymbol{k})+D_{+1}(\boldsymbol{k}+\boldsymbol{k}_0)H^*(\boldsymbol{k}+\boldsymbol{k}_0)+D_{-1}(\boldsymbol{k}-\boldsymbol{k}_0)H^*(\boldsymbol{k}-\boldsymbol{k}_0))+D_{+2}(\boldsymbol{k}+2\boldsymbol{k}_0)H^*(\boldsymbol{k}+2\boldsymbol{k}_0)+D_{-2}(\boldsymbol{k}-2\boldsymbol{k}_0)H^*(\boldsymbol{k}-2\boldsymbol{k}_0)\ /(\text{abs}(H(\boldsymbol{k})))^2+(\text{abs}\big(H(\boldsymbol{k}+\boldsymbol{k}_0)\big))^2+(\text{abs}\big(H(\boldsymbol{k}-\boldsymbol{k}_0)\big))^2+(\text{abs}\big(H(\boldsymbol{k}+2\boldsymbol{k}_0)\big))^2+(\text{abs}\big(H(\boldsymbol{k}-2\boldsymbol{k}_0)\big))^2+w^2\ )$$

2-46

Where in 2-46 w is the wiener filter parameter and the symbol * is the complex conjugate and abs represent the absolute value or modulus.

Chapter Three

Analysis of Non-linear Structured Illumination Microscopy (SIM)

3.1 Theory of non-linear structured illumination microscopy

As stated in chapter two, the linear structured illumination establishes a linear relationship between the excitation intensity (I_{ex}) and the emission intensity (I_{em}).

Mathematically, we can write:

$$I_{ex} = kI_{em} \qquad 3\text{-}1$$

Where k is a proportionality constant that ranges from zero to one. k defines how much of fluorescence is obtained from an excitation. In ideal case, this will be 1 but that's a mirage. The sample is a distribution of fluorophores ($F\ (r)$).

Hence, the overall fluorescence is given by:

$$I_{ex} = kF(r)I_{em} \qquad 3\text{-}2$$

Also, in chapter two it was stated that the maximum spatial frequency that can be transmitted is given by $2NA/\lambda_{ex}$ where λ_{ex} is the wavelength of the excitation light. It is clear, the maximum resolution is twice of that of the conventional microscope, and it is limited by diffraction

(wavelength of the excitation light). In Non-linear SIM, a non-linear relationship is established between the $I_{ex}\,(r)$ and the $I_{em}\,(r)$ which introduces higher spatial frequencies in $I_{em}\,(r)$.As shown in Fig. 3-1 [10], with more non-linearity there is more high harmonic components which means we have more OTF support copies that can be used to get more high frequency information. The level of resolution improvements depends on number of high harmonics terms that is captured via the non-linearity mechanism used and the resolution for non-linear SIM is therefore theoretically unlimited [32].

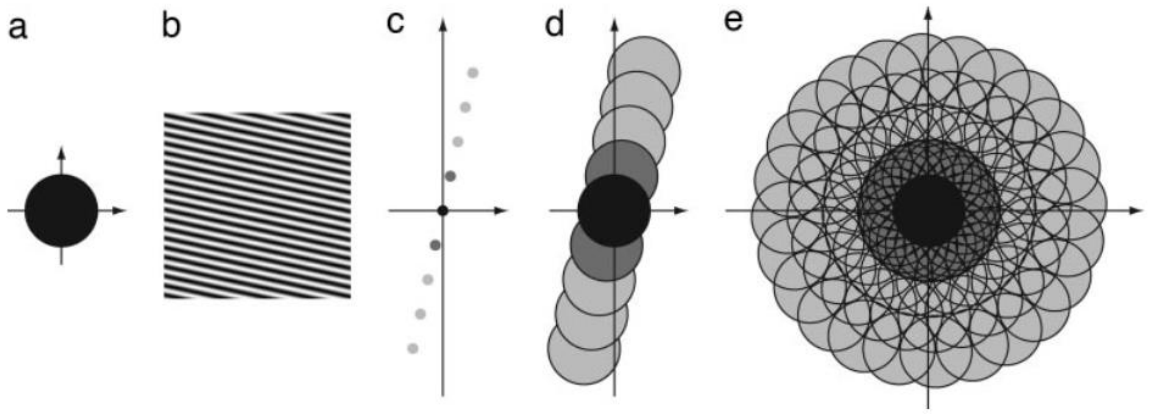

Figure 3-1 [31]. Nonlinearity of SIM. a, black colored is the normal OTF support of conventional microscope.b,A sinusoidal pattern for non-linear SIM. c,black and dark grays represents the average and modulation of the pattern. Under linear SIM these black and dark grays constitute the zero and first orders of the image. In non-linear SIM we have higher orders as shown by the three lighter grays which are the three lowest harmonics.d, region of support for conventional microscope in black, linear SIM (dark grays) and non-linear SIM ligher grays for three lowest harmonics.e, Observable regions for different pattern orientations. A much larger region of spatial frequencies can be seen resulting in higher resolution.

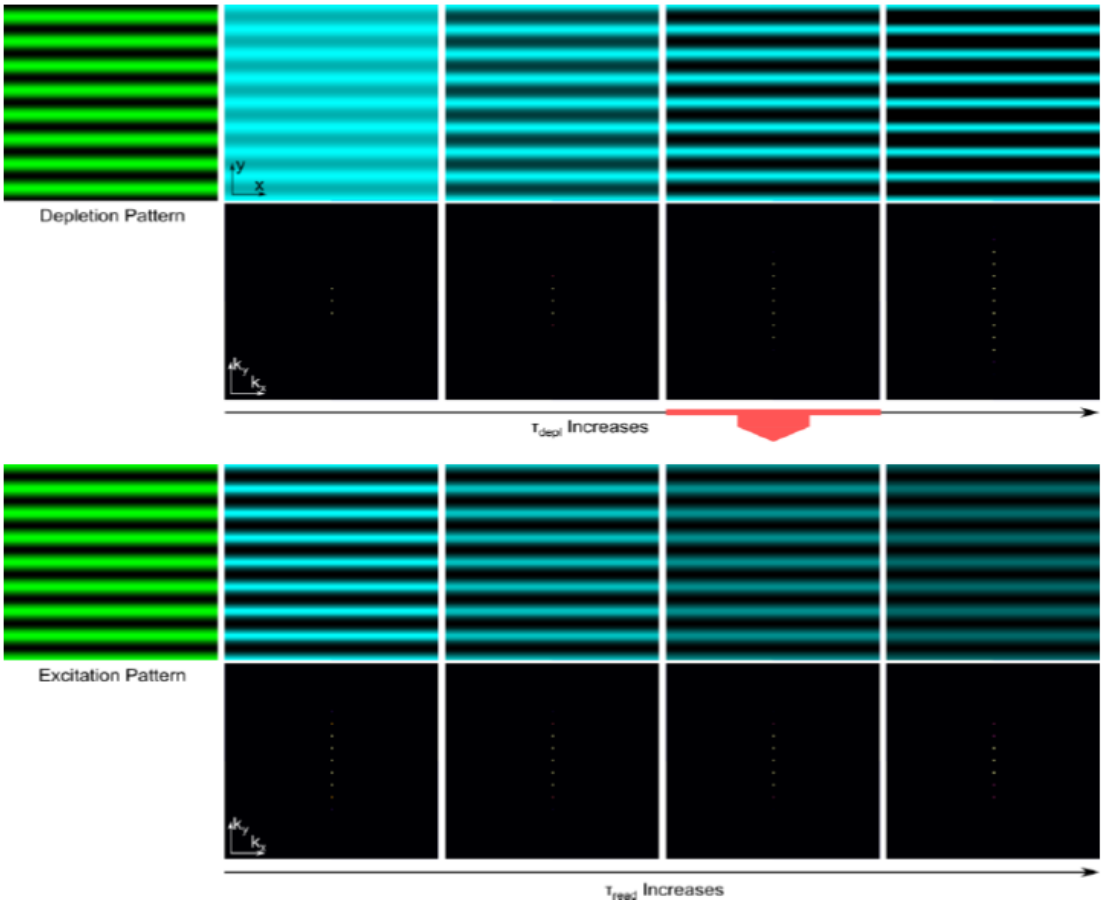

Figure 3-2 [10]. Pictorial illustration of non-linear SIM using depletion pattern. Top rows show the fluorophores that were on when the depletion pattern was on for T_{depl}.As T_{depl} increases we get more higher order harmonics. Bottom row is the fluorophores that were on during readout starting from the red arrow shown. As $T_{readout}$ increases we have fewer harmonics, but the image captured by the camera will still contain high order harmonics since it is an integral over the all the time the camera is exposed to fluorescence.

3.2 Mathematical analysis of non-Linear Structured Illumination Microscopy

To establish a non-linear relationship between the emission and illumination two approaches are commonly used: saturation of the fluorophore excited state employed in saturated structured illumination microscope and using the photo switching properties of reversible photo switchable fluorophores such as rsEGFP2.Although, the first method has achieved high sub-

diffraction resolution that is less than 50 nm it involves saturating the excited fluorophores using illumination with peak intensities of the order of 10 MW/cm^2 which can cause photodamage of samples and make it unsuitable for live cell imaging. The second approach which I am going to discuss more about in this thesis uses the ability of rsEGFP2 to be switched repeatedly between a non-fluorescent off states and a fluorescent on state to introduce a non-linear relationship between the illumination and emission. With a low light intensity that's of the order of 10 W/cm^2 a non-linear response was generated whose resolution was approximately 40 nm on purified microtubules labeled with Dronpa [22]. One method that is used to establish a non-linear relationship between emission and illumination by exploiting properties of rsEGFP2 is the pattern depletion method (shown in figure 3-2 [10]). In this method, all the fluorophores are excited by a short wavelength light (405 nm, violet) and a subset of these are then de-energized by a long wavelength light (488 nm, blue) using an illumination pattern given by:

$$I_{off}(r) = I_0/2[1 - \cos(2\pi kr + \phi) \quad \text{3-3}$$

Where $k, r, \phi \; and \; I_0$ are the wavenumber, spatial co-ordinates, phase difference and peak intensity respectively. If this deactivation light is of the duration t_{off},then the rsEGFP2 that remains on during this duration is given by:

$$I_{on}(r) = 1/(1 + \left(I_{off}(r).\frac{t_{off}}{\delta_{dep}}\right)) \quad \text{3-4}$$

Where δ_{dep} is the characteristics decay constant of depletion.

To read out the image an excitation light of the same period but with a phase shift of $180^0 + \phi$ is used. Hence, the readout is a sinusoidal pattern given by:

$$I_{readout}(r) = I_0/2(1 + \cos(2\pi kr + \phi)) \quad 3\text{-}5$$

As before the fluorescence that remains on when this read out light is on for a duration(t) is given by:

$$I_{read}(r,t) = 1/(1 + (I_{readout}(r).\frac{t}{\delta_{dep}})) \quad 3\text{-}6$$

If T is the total amount of time that the image sensor of the camera is exposed to fluorescence. Then the overall fluorescence captured by the camera is the integration of the multiplication of the readout intensity and the fraction of fluorophores that were on during the read out. This is given by:

$$I_{im}(r) = \int_0^T I_{on}(r).I_{readout}(r).I_{read}(r,t)dt$$

$$I_{im}(r) = I_{readout}(r)/(1 + \left(I_{off}(r).\frac{t_{off}}{\delta_{dep}}\right)) \int_0^T 1/(1 + (I_{readout}(r).\frac{t}{\delta_{dep}})) \quad 3\text{-}7$$

From binomial expansion:

$$\frac{1}{1+x} = 1 - x + x^2 - x^3 + \ldots\ldots \quad \text{3-8}$$

$$e^x = 1 + x + \frac{x^2}{2} + \frac{x^3}{6} + \cdots \quad \text{3-9}$$

Also, the emission E(r) is given by:

$$E(r) = 1/\delta_{dep} \int_0^T I_{readout}(r) e^{-\frac{t}{I_0 I_{readout}(r)}} S(r) dt \quad \text{3-10}$$

Where $S(r)$ is the fluorophore distribution. Also, we can define the saturation factor (η) as the ratio of exposure times(t) to δ_{dep} which determines the level of linearity. The higher the saturation the higher the orders of non-linearity and the higher the resolution as shown in Fig. 3-3[21].

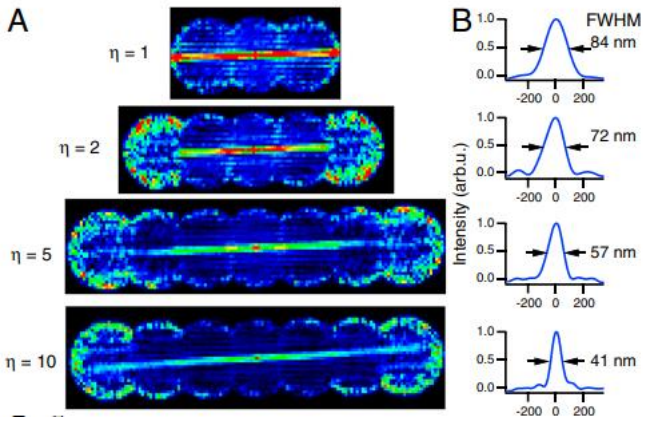

Figure 3-3 [21]. Relationship between saturation factor, higher orders, and resolution. A, shows with more saturation factor there is higher orders and seen with more copies of the OTF and B, shows more resolution.

Comparing 3-8 to the terms in 3-7 it is clear that $1/(1+(I_{readout}(r).\frac{t}{\delta_{dep}}))$ and $1/(1+\left(I_{off}(r).\frac{t_{off}}{\delta_{dep}}\right))$ are of this form and therefore constitute the non-linearity in $I_{im}(r)$. Also, comparing the $e^{-\frac{t}{I_0 I_{readout}(r)}}$ to 3-9 we can see the non-linearity due to higher orders define by the powers.

As stated before, the resolution of non-linear SIM depends on the order of harmonics included in the final image. In 2D non-linear SIM, to capture the first higher-order harmonics (at least 2nd and 3rd order) the patterns are shifted in steps of $2\pi/5$ and rotated for 6 angles $(0^0, 36^0, 72^0, 108^0, 144^0, 180^0)$ for each step to capture an isotropic space and to obtain a total of 5 (phase) by 6 (angles)=30 raw image frames.

3.3 2D non-Linear SIM Image Reconstruction

2D non-linear SIM image reconstruction is like that for the linear SIM. Since, for each image we need five phases then we can define the phase (ϕ) in steps of 2π/5 and it is given by:

ϕ= [0, 2π/5, 4π/5, 6π/5, 8π/5] 3-9

Where, ϕ_0=0, ϕ_1=2π/5, ϕ_2=4π/5, ϕ_3=6π/5, ϕ_4 =8π/5.

Also, as before:

The image captured by the camera can be defined as:

$$D(\boldsymbol{k})=O(k)H(k) + O(k + k_o)e^{i\phi}H(k) + O(k - k_o)e^{-i\phi}H(k) + O(k + 2k_o)e^{2i\phi}H(k) + O(k - 2k_o)e^{-2i\phi}H(k) \quad 3\text{-}10$$

Where $D_0= O(k)H(k)$, $D_1=O(k + k_o)H(k)$, $D_{-1}=O(k - k_o)H(k)$, $D_2 = O(k + 2k_o)H(k)$ $and\, D_{-2} = O(k - 2k_o)H(k)$

For each phase we can write:

$$D_{\phi0}=D_0+D_1e^{i\phi0}+D_{-1}e^{-i\phi0}+D_2e^{2i\phi0} + D_{-2}e^{-2i\phi0}$$

$$D_{\phi1}=D_0+D_1e^{i\phi1}+D_{-1}e^{-i\phi1}+D_2e^{2i\phi1} + D_{-2}e^{-2i\phi1}$$

$$D_{\phi2}=D_0+D_1e^{i\phi2}+D_{-1}e^{-i\phi2}+D_2e^{2i\phi2} + D_{-2}e^{-2i\phi2}$$

$$D_{\phi3}=D_0+D_1e^{i\phi3}+D_{-1}e^{-i\phi3}+D_2e^{2i\phi3} + D_{-2}e^{-2i\phi3}$$

$$D_{\phi4}=D_0+D_1e^{i\phi4}+D_{-1}e^{-i\phi4}+D_2e^{2i\phi4} + D_{-2}e^{-2i\phi4}$$

In matrix form we can write:

$$\begin{bmatrix} D_{\phi 0} \\ D_{\phi 1} \\ D_{\phi 2} \\ D_{\phi 3} \\ D_{\phi 4} \end{bmatrix} = \begin{bmatrix} 1 & e^{i\phi 0} & e^{-i\phi 0} & e^{2i\phi 0} & e^{-2i\phi 0} \\ 1 & e^{i\phi 1} & e^{-i\phi 1} & e^{2i\phi 1} & e^{-2i\phi 1} \\ 1 & e^{i\phi 2} & e^{-i\phi 2} & e^{2i\phi 2} & e^{-2i\phi 2} \\ 1 & e^{i\phi 3} & e^{-i\phi 3} & e^{2i\phi 3} & e^{-2i\phi 3} \\ 1 & e^{i\phi 4} & e^{-i\phi 4} & e^{2i\phi 4} & e^{-2i\phi 4} \end{bmatrix} \begin{bmatrix} D_0 \\ D_1 \\ D_{-1} \\ D_2 \\ D_{-2} \end{bmatrix} \quad 3\text{-}11$$

Where A==$\begin{bmatrix} 1 & e^{i\phi 0} & e^{-i\phi 0} & e^{2i\phi 0} & e^{-2i\phi 0} \\ 1 & e^{i\phi 1} & e^{-i\phi 1} & e^{2i\phi 1} & e^{-2i\phi 1} \\ 1 & e^{i\phi 2} & e^{-i\phi 2} & e^{2i\phi 2} & e^{-2i\phi 2} \\ 1 & e^{i\phi 3} & e^{-i\phi 3} & e^{2i\phi 3} & e^{-2i\phi 3} \\ 1 & e^{i\phi 4} & e^{-i\phi 4} & e^{2i\phi 4} & e^{-2i\phi 4} \end{bmatrix}$

To construct the image, we need to obtain the images $D_0, D_{-1}, D_1, D_{-2}, D_2$ hence we multiply the inverse of A by images for each phase.

$$A^{-1} = \begin{bmatrix} 1 & 1 & 1 & 1 & 1 \\ e^{i\phi 0} & e^{i\phi 1} & e^{i\phi 2} & e^{i\phi 3} & e^{i\phi 4} \\ e^{-i\phi 0} & e^{-i\phi 1} & e^{-i\phi 2} & e^{-i\phi 3} & e^{-i\phi 4} \\ e^{2i\phi 0} & e^{2i\phi 1} & e^{2i\phi 2} & e^{2i\phi 3} & e^{2i\phi 4} \\ e^{-2i\phi 0} & e^{-2i\phi 1} & e^{-2i\phi 2} & e^{-2i\phi 3} & e^{-2i\phi 4} \end{bmatrix} \quad 3\text{-}12$$

Hence, the reconstructed images are:

$$\begin{bmatrix} D_0 \\ D_1 \\ D_{-1} \\ D_2 \\ D_{-2} \end{bmatrix} = A^{-1} \begin{bmatrix} D_{\phi 0} \\ D_{\phi 1} \\ D_{\phi 2} \\ D_{\phi 3} \\ D_{\phi 4} \end{bmatrix} \quad 3\text{-}14$$

3.4 Previous switching results with non-linear SIM

Previous works with non-linear SIM using rsFPs was done by Rego et al. [21] using Dronpa. Dronpa was activated using violet light at (~405 nm) and deactivated using blue light at

(~488 nm) to elicit fluorescence at (~510 nm). Deactivation characteristics of Dronpa was compared using two antifade reagents: PHEM (PurMa Hybridoma Essential Media) and PPD (phenylenediamine). Fig.3-4A shows the deactivation (off rate) characteristics of Dronpa at different illumination (488 nm) powers. The off-rate characteristics of Dronpa is linear with illumination and with no significance difference between that of PPD and PHEM at a PH of 6.9. The switch fatigue of Dronpa was also compared in Fig.3-4B. At roughly 15cycles fluorescence drop to $1/e$ of their initial value with PHEM. However, the switching cycles survived before photobleaching was improved with PPD. At $5\ mM$ of PPD and with light intensity of $5\ Wcm^{-2}$ Dronpa was observed to switch 60-70 times. Fig.3-4C compared the normalized intensity to the off-state intensity (background). The emission fluorescence intensity (circles) was found to be roughly 50 times greater than that of the off state(plus). Also, the off-state intensity was approximately constant and below 20% of maximum fluorescence.

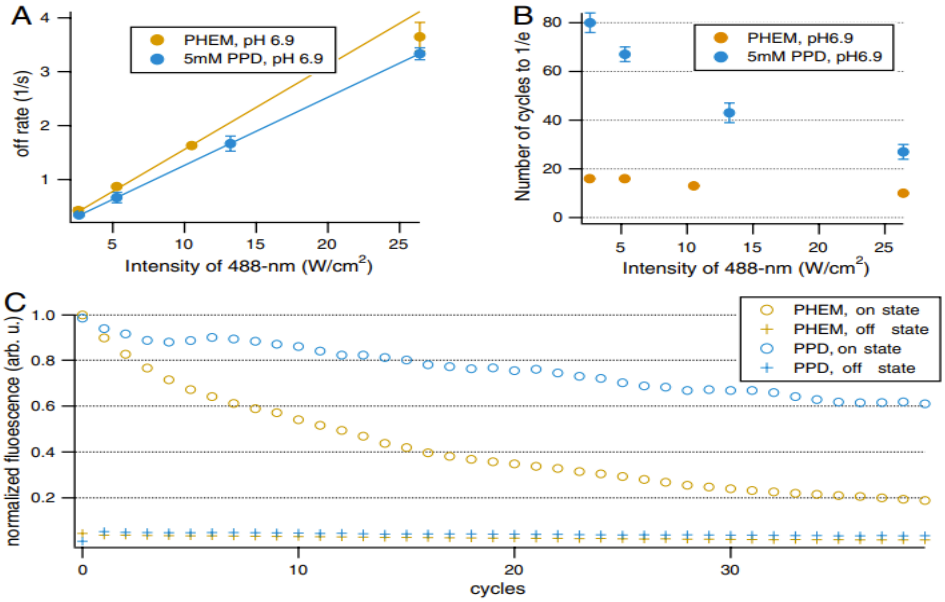

Figure 3-4. Comparison of switching behavior of Dronpa with PPD (blue) and PHEM (orange). A, off rate characteristics of Dronpa is linear with illumination. B, Switch cycles of Dronpa is improved from 15cycles to approx. 80 cycles at lower illumination using PPD. C, on state fluorescence is roughly 50times greater than off state fluorescence(background) and with background roughly constant.

Chapter Four

Methods and Discussion of Results

4.1 Review of the research objectives

As discussed in chapter one the key objective of this research is to characterize the reversibly photo switchable Enhanced Green Fluorescent Proteins 2 (rsEGFP 2) which is a genetically enhanced version of Green Fluorescent Proteins (GFP) [18]. I will measure the fluorescence of rsEGFP2 as a function of time under different conditions and determine the switch fatigue, fluorescence decay constant, variation of peak fluorescence, the activation time constant, and the ratio of off-state fluorescence to maximum fluorescence. By obtaining raw data computationally and analyzing the data to characterize rsEGP 2 using these parameters, we can establish the suitability of rsEGFP2 for non-linear Structured Illumination Microscopy (SIM).

Also, these parameters influence the resolution of the final image. Switching Fatigue is defined as the ability of rsEGFP2 to survive several on-off switching cycles before photobleaching. The fatigue in this context connotes a negative meaning in that high fatigue means fewer switching cycles. Contextually, a positive way to look at it is a higher switch fatigue resistance. The higher resistance to switch fatigue, the better the ability of rsEGFP2 to survive more cycles. The decay constants measure how fast the fluorescence turns off when exposed to the excitation light at 488nm. The fluorescence (I) is related to the background (B) and amplitude (I_0) by the equation:

$$I = I_0 exp^{-t/\tau} + B \quad \text{4-1}$$

Where τ is the activation time constant in seconds. The reciprocal of τ is the decay constant in inverse seconds. The maximum fluorescence for a cycle is given by:

$$I_{max} = I_0 + B \quad \text{4-2}$$

Where I_0 and B are the amplitude and the background (off -fluorescence) respectively for the cycle. Then the ratio of B to I_{max} for a cycle is termed the ratio of off-fluorescence(background) to maximum fluorescence for that cycle. Fig.4-1 is a plot of the simulated output of the arduino code in appendix A for a pulse cycle. The 405 nm laser is turned on for a duration (1 millisecond in this case) and then turned off and the 488 nm laser is turned on for a longer duration (46 milliseconds). The fluorescence is read out by the camera over the duration of the pulse. In the next cycle the 405 nm laser is turned on for 2 milliseconds (twice the previous) and the 488 nm laser is turned on for 45 milliseconds. The duration of the 405 nm follows an arithmetic progression with a common difference of 1 millisecond and a first term of 1 millisecond. So, the 20^{th} cycle has 405 nm laser duration of 20milliseconds and the 488 nm of 22 ms.

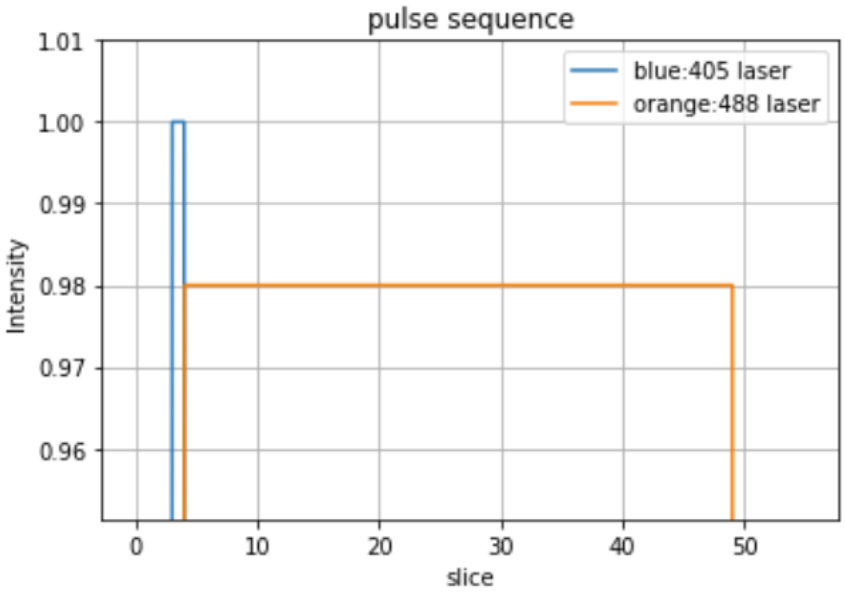

Figure 4-1. Pulse sequence of the 405 nm and 488 nm lasers in the first cycle. The 405 nm laser was turned on for 1 ms and then turn off. The 488 nm laser was then turned on for a longer duration (shown here is 46 ms) to read out fluorescence. For the next cycle the 405 nm laser is turned on for twice the previous duration and the 488 nm laser is also turned on for a 45 ms. The process continues until the final cycle. For example, if the exposure time for 1st cycle is 1 ms,2nd is 2 ms in that order until the 20th cycle which is 20 ms and in every case the 488 nm is turned on for longer period to read out fluorescence.

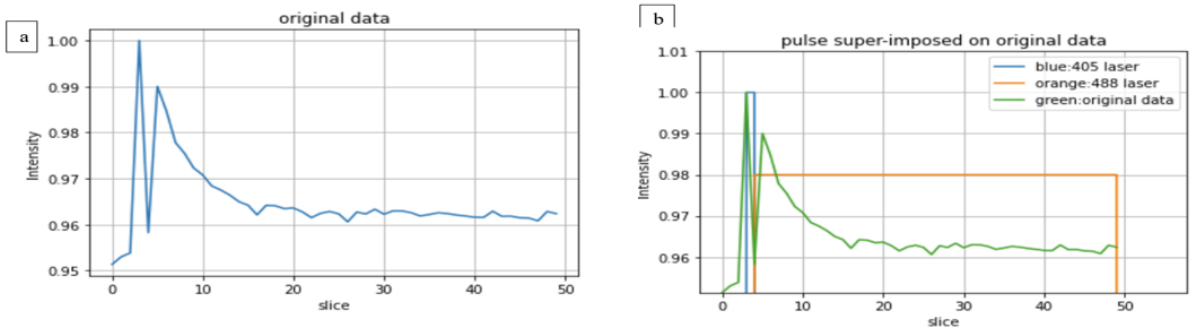

Figure 4-2. Pulse sequence super-imposed on original data. a, normalized intensity of the original data. b, pulse super-imposed on the original data. The 405 nm laser has a duration of 1 ms and 488 laser has 49 ms to read out fluorescence. An exponential fit is done to the fluorescence to calculate the decay constant and a plot of the fluorescence against exposure time is also done to characterize the switching fatigue.

A practical example of the pulse sequence is shown in figure 4-2 (above) which is a cycle (a slice) of an experiment that was carried out with an exposure time of 1 ms, 488 laser power of 5 mW and 405 laser power of 4 mW with U2OS cells tagged with rsEGFP2. There is a total of 40 cycles with 50 slices per cycle. Fig.4-2(b) shows the 405 nm laser and 488 nm laser pulses and the fluorescence emission signal. The exposure time (0.001s) increases by a multiple of image segment (1-40 segments) with 50 slices per segments. So, exposure for 1st segment is $0.001 * 1\ s$,second is $0.001 * 2\ s$, in that order until the 40th segments. According to the python code in appendix F, if we define the normalized fluorescence (C_n) as:

$$C_n = C_{max}^{-1}(A * exp^{-ax} + B * exp^{-bx}) \qquad 4\text{-}3$$

Where C_{max}^{-1} is reciprocal of the maximum fluorescence which is A+B and a, b are time constants and x is a slice. The parameters A, B, a and b are returned as the optimized parameters in the curve fit function in python. By calculating the values of C_n for every slice I can obtain the amount of fluorescence remaining for a slice which is used to quantity the switch fatigue.

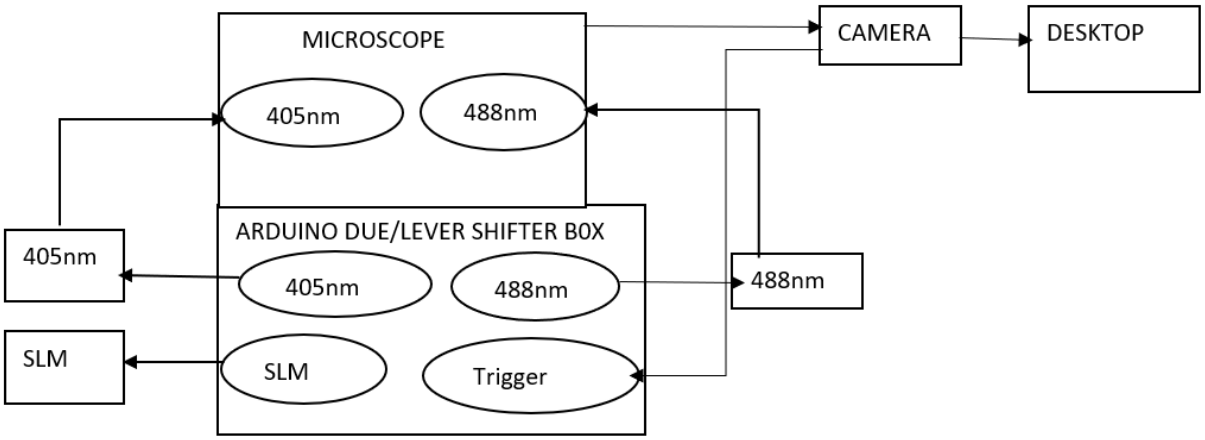

Figure 4-3. A simplified block diagram of the overall project set up. Inputs from the camera to the level shifter triggers the Arduino and consequently outputs signal from the 405nm terminal,488nm terminal and SLM terminal to control the 405nm laser, 488nm laser and the SLM (Spatial Light Modulator) . The signals are then fed to the sample on the microscope stage to energize the fluorophores and to excite fluorescence. The output from the camera (input from the microscope) is fed to the Desktop where raw data is characterized.

4.2 Overview of the hardware design

A general overview of the design is shown in the block diagram in figure 4-3 above. A 5 V trigger signal from the camera is shifted down to 3.3 V by the level shifter and then fed into a digital input pin of the Arduino. A 3.3 V output signal is then obtained from the digital output pins of the arduino and used to control the 405 nm laser,488 nm laser and the SLM (Spatial Light Modulator). The output signals from the arduino are used to activate the fluorophores with the 405 nm laser and to excite fluorescence with the 488 nm laser. Images are then captured by the camera and raw data are obtained computationally via the desktop. The materials in the block diagrams are explained in the subsequent sections.

4.3 Materials

A schematic of the connections inside the box (Figure 4-4) enclosing the Arduino and the level shifter is shown in Figure 4-5 below. Materials/Equipment used in the schematics are explained below:

4.3.1 Arduino Due

The Arduino Due board is based on a 32-bit ARM core microcontroller. It has 54 digital input/output pins, 12 analog inputs, 2 DAC (digital to Analog pins) and 2 CAN (Controller Area Network) buses, 4UARTs (hardware serial ports), an 84MHz clock, a USB OTG capable connection, a power jack, an SPI header, a JTAG header, a reset button, an erase button and a 96 kb of SRAM.Also,12 of the 54digital pins can be used to generate a pulse. Each of the digital pins accepts voltage up to 3.3 V and the nominal input voltage is within the range of 7-12V. The external trigger signal from the camera is used as the digital input to the arduino microprocessor which keeps track of the number of frames and turns on and off the 405 and 488 lasers.

4.3.2 Logic level converter

The logic level converter (BOB-12009, Spark Fun) is a bi-directional voltage levels shifter. It safely steps down a 5 V to 3.3 V and a 3.3 V to 5 V. It can also work with lower voltage devices like 2.8 V and 1.8 V. It has four pins on the low voltage (LV1, LV2, LV3, LV4) and high voltage (HV1, HV2, HV3, HV4) sides that steps voltages up or down. There is a high voltage (HV) and low voltage power (LV) power input pins which accepts up to 5 V and 3.3 V respectively relative to ground (GND) pins.

4.3.3 CAMERA

The camera is an Andor Sona 4.2B-6. It is a 4.2 Megapixel (back illuminated) camera that operates in a 12-bit low noise mode using correlated multi-sampling to reduce read noise. The camera outputs 5 V signal when the camera is being exposed which is stepped down by the level shifter to 3.3 V to trigger the Arduino. The frame rate increases as the region of interest decreases.As for example,the maximum frame rate for a region of interests of 2048 by 2048 and 1200 by 1200 are 43 frames per second and 74 frames per second respectively.The camera frame rate for the experiment is 500 frames per second and the maximum frame rate obtained for a region of interest of 64 by 64 is approximately 600 frames per second with a mean frame rate of approximately 0.00137 second. The exposure time for the experiment is 1 ms. These parameters are specified in the python code in appendix A.

Figure 4-4. Box containing arduino and level shifters. Terminals for the 405 nm laser,488 nm Laser and the Camera also shown.

4.3.4 Lasers and Spatial Light Modulator (SLM)

The lasers are (Cyan 488 nm-Spectra-Physics and 405 nm Coherent OBIS Lasers). The SLM is a $2048 * 1536$ pixels light modulator with pixel size of $82\ \mu m$(Forth Dimension QXGA-3DM).

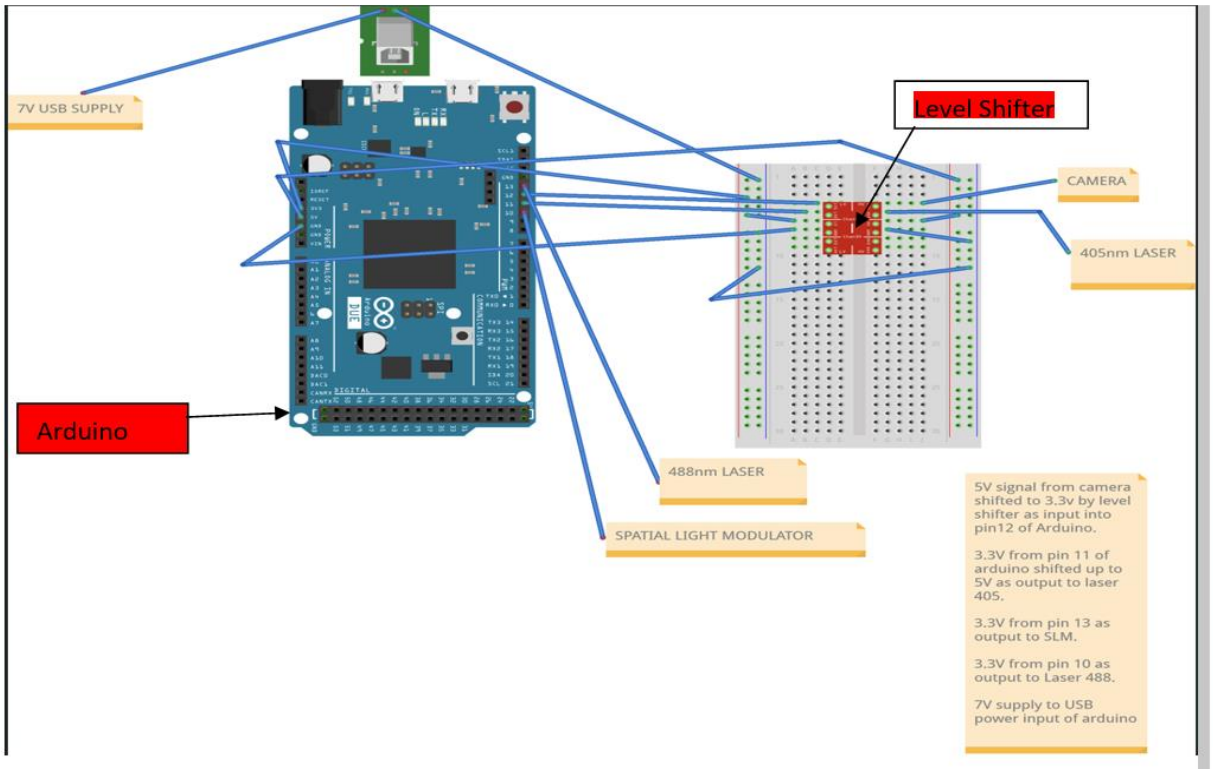

Figure 4-5. Schematics of connections inside the box showing the arduino due and level shifter. Brief connections explanations are shown in the text box.

The materials not described in Figure 4-5 but are in figure 4-3 are explained below.

4.3.5 Microscope

The microscope is an Olympus IX71 with a Prior Proscan XY stage and a Prior 200-micron travel NanoScan Z stage for sample movement and focusing. The sample (actin tagged with rsEGFP 2 inside U2OS cells) is placed on the stage.

4.3.6 Desktop Computer

The desktop computer is a Dell x64- based PC with an intel processor whose speed is 2.80 GHz. Raw data are obtained from the computer and then characterized using different computational methods.

4.9 Methods

The fluorophore characterization involves two procedures the hardware (electronics connections) and the sequence of steps in performing the experiment.

4.9.1 Electronics connections

The electronics connections provide a detailed explanation of the schematics in Fig.4-3. A 5 V signal from the auxiliary 1 output of the camera supplies the HV1 input of the level shifter via the camera terminal shown in the block diagram. This are then shifted down to 3.3 V via the LV1 output of the level shifter. This output is fed into the digital pin (12) of the Arduino due. The 3.3 V outputs from the digital pin (11) of the Arduino is fed into the LV2 of the level shifter and then shifted up to 5 V via the HV2 of the level shifter. This 5 V output of the level shifter is used to control the 405 nm Laser. The 3.3 V outputs from digital pin (13) and 10 are used to control the 488 nm Laser and the Spatial Light Modulator respectively. The LV and HV of the level shifter are powered with 3.3 V and 5 V respectively and their respective GND terminals are

connected to the arduino ground pins. The Arduino due is powered by a USB port on the desktop.

4.9.2 Sequence of steps

Step 1: Put the sample (U20S cells) on stage of the Olympus Microscope.

Step 2: Set the power of the 405 nm laser through the OBIS Coherent Software (Fig. 4-6).

Step 3: Adjust the half wave plate to vary the power of the 488 nm laser and record the power of the 488 nm laser through the power meter (Fig.4-7).

Step 4: Run the Arduino code in appendix A. This algorithm controls the sequence of trigger signals, 405-laser signals and 488-laser signals which are outputs of the Arduino.

Step 5: Run the Python code in appendix B. This program is used to set the exposure time and the frame rate of the 5 V trigger signal from the camera). Exposure time used for the experiment is 1milliseconds. The program is also used to read the camera image.

Step 6: Observe the raw values and a slice of it to accurately determine the camera background. The background is where the 488 nm laser is off, and this is observed as lowest value on the plot when fluorescence is read out.

Step 7: This step involves loading the image into ImageJ removing the background by these sequences: process >>>> math >>>> subtract and using the macros algorithm in appendix C to extract the raw values from image frames and convert them to a csv file. To convert to a csv file, we add a .csv extension to the file name.

Step 8: Use the algorithm in appendix D and appendix E to characterize the rsEGFP2. Appendix D algorithm extract the mean intensity for the odd slices and even slices and provide a double exponential fit for the respective mean intensities. The switch fatigue is then characterized via a plot of the exponential fits of the mean intensities against slices. Appendix E algorithm calculates the time constants, background, and the ratio of background to maximum intensities for each cycle of the data. It provides a plot of the time constants, background, and the ratio of background to maximum intensities for the entire cycle.

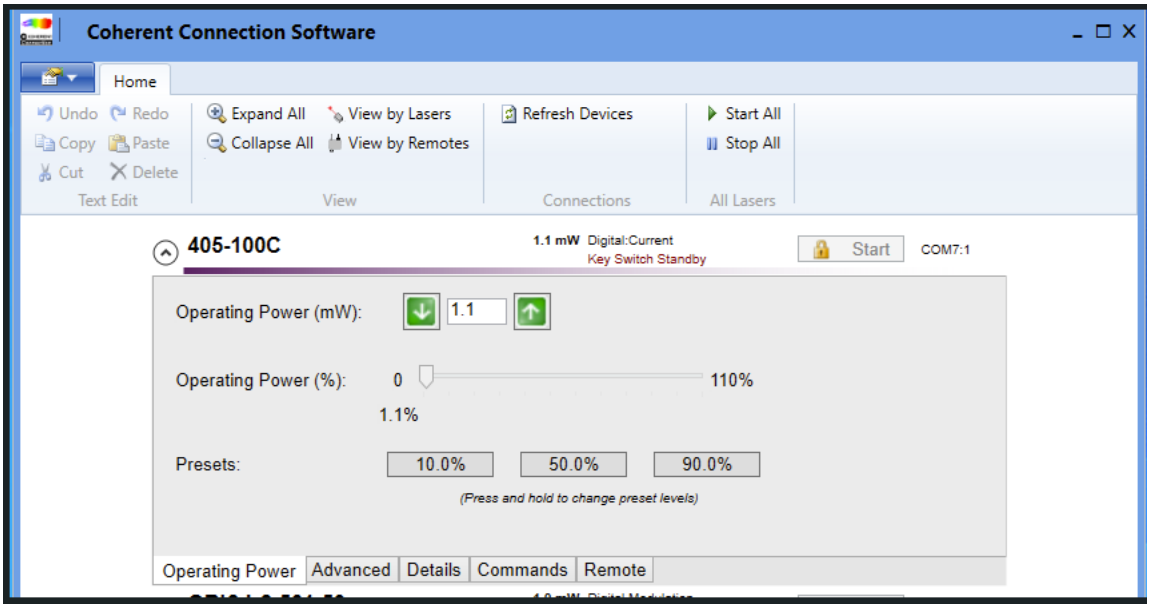

Figure 4-6. OBIS Coherent Software for setting the power of the 405 nm Laser.

Figure 4-7. PM100D (power meter) from THORLABS to measure the 488 nm Laser power.

4.10 Sample Protocols

The sample in brevity is U20S cells labelled with rsEGFP2. The sample protocols are summarized below:

4.10.1 U2OS cell culture protocols:

A. ***Materials required:***

U2OS cells

DMEM medium (cytiva #SH30243.01)

Penicillin-streptomycin solution

Fetal bovine serum (FBS)

Phosphate-buffered saline (PBS)

Trypsin-EDTA solution

Cell culture flasks

Centrifuge tubes

Liquid nitrogen

B. Growth medium: DMEM (GIBCO # 11960) + 10% FBS + 1% penicillin-streptomycin

C. Thawing U2OS Cells:

1.Take out the U2OS stock vial from liquid nitrogen and thaw it at room temperature. Resuspend thawed cells in 1000 ul growth media and transfer cells into 25 ml cell culture flasks. Cells are grown in a 36.7°C incubator with humidified atmosphere of 5% CO2.

D. Subculturing of U2OS Cells:

1. Aspirate growth media from the cell culture flask.
2. Remove the culture medium and rinse the cells with sterile PBS.
3. Add 500 ul of Trypsin-EDTA solution and allow the cells to incubate in the 37°C incubator until cells detach (approximately 5 min).
4. Add 2000 ul of fresh growth media to neutralize the trypsin and collect cells in a centrifuge tube (the ratio of Trypsin-EDTA solution and growth media is 1:4).
5. Spin at 1500 rpm for 5 minutes.
6. Aspirate supernatant and add 1000 ul fresh growth media to resuspend the cells.
7. Transfer 15 ul cell suspension liquid to a new culture flask with 5000 ul fresh medium and place in a 36.7°C incubator at 5% CO2.

E. Freezing of U2OS Cells:

1. Aspirate growth media from the cell culture flask.
2. Add 500 ul of Trypsin-EDTA solution and incubate in the 37°C incubator until cells detach.
3. Add 2000 ul of growth media with 5% DMSO and collect cells in a centrifuge tube.
4. Spin at 1500 rpm for 5 minutes.
5. Aspirate supernatant and resuspend cells in growth media with 5% DMSO.
6. Transfer cells to cryovials and store in liquid nitrogen.

4.10.2 rsEGFP2 U2OS cell transfection protocols:

A. Materials required:

U2OS cells

rsEGFP2 plasmid DNA

iBidi 35mm glass bottom dish

Fibronectin human plasma

Plasmid DNA (containing the gene of interest)

Polyethylenimine (PEI) transfection reagent

Growth medium (DMEM (GIBCO # 11960) + 10% FBS + 1% penicillin-streptomycin)

Opti-MEM medium

Phosphate-buffered saline (PBS)

C. Transfection protocols:

1. Use 1000 ul of 0.1% PBS diluted fibronectin human plasma to coat the 35 mm iBidi dish for 30 min at room temperature.
2. Aspirate the fibronectin human plasma and add 100 ul U2OS cell suspension liquid into iBidi dish with 1000 ul fresh growth medium and plate the cells in a 36.7°C incubator at 5% CO2 for 18-24 hours before transfection. An appropriate seeding density should be used so the cell culture plate is 90-95% confluent at the time of transfection.
3. Rinse the cells with sterile PBS to remove residual culture media, add 1000 ul fresh growth medium.
4. Tube A: Prepare plasmid DNA by diluting 3 µg of plasmid DNA in 50 µL of Opti-MEM medium in a sterile tube.
5. Tube B: Prepare transfection reagent by adding 6 µL of PEI to 50 µL of Opti-MEM medium in a sterile tube. Vortex gently.

6. Add the transfection reagent solution (tube B) to the tube containing plasmid DNA (tube A), and vortex immediately. Spin down gently and allow the complexes to form for 10 minutes at room temperature.
7. Add 100 µL of the complex mixture (tube A+B), dropwise, to each well containing cells and medium. Mix gently by swirling the plate. Incubate the cells at 36.7°C incubator at 5% CO2 for 24 hours.
8. Cells were imaged 24–30 hours after transfection.

4.11 Computational (Desktop) Methods

The algorithm in appendix D uses a curve fit function and the pandas library in python. The curve fit function is based on minimizing errors by using the least squares method. It returns two parameters popt (optimized parameters of the exponential function I am fitting to the mean intensity) and the covariance matrix (pcov) which is an estimate of the errors in the parameters. The exponential fit has amplitude A and B and decay constant a and b for the even(activation) slices and the odd (depletion) slices. To keep the decay constants positive a matrix called bounds can also be provided as an argument to the exponential fits. The algorithm in D is written to superimpose the exponential fit over the original data to have a pictorial view of the extent to which the fits match the original data as shown in Figure 4-8a and b for the activation slices (even slices) and the depletion slices (odd slices) respectively. From the exponential fits I use the algorithm in appendix F to determine the amount of intensity remaining for a particular cycle. This provides information about the switching fatigue as shown in Table 4-1,4-2 and 4-3. The algorithm in appendix G provide information on how the decay constant is changing for the even slices(activation) and odd slices (depletion) which also provides information about their switch fatigue. These are shown in Fig.4-9.

The algorithm in appendix E defines an exponential function that returns the amplitude (A) , Background (B) and the time constant (tau) . Also, like algorithm D it also uses the curve fit function and the pandas library in python. To characterize rsEGFP 2 I provide a plot of exposure time against the time constant as shown in Fig. 4-11, exposure time against the peak intensity as shown in Fig.4-12, exposure time against background as shown in Fig.4-13 and the exposure time against the fraction of max intensity as shown in Fig.4-14. The quality of the curves depends on carefully choosing the index values (index stop and index start of the original data) .

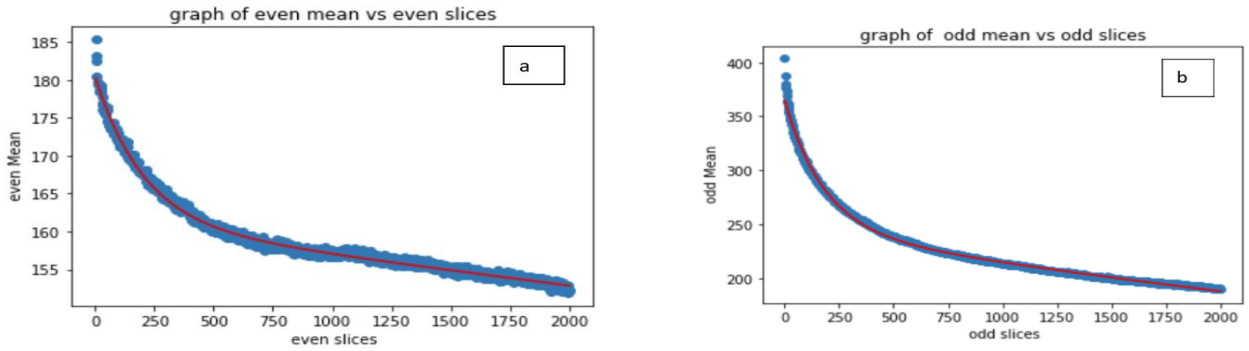

Figure 4-8. Non-normalized fits to the original data.Blue and Red are the non-normalized original data and exponential fits respectively. a, is the even (activation) slices and b, is the odd (depletion slices) .

4.12 Image Processing with ImageJ

Fiji ImageJ is used to view the image, extract intensity values from the image frames and convert a data file of the image to a csv file. The process involves observing the entire data through a plot of the fluorescence intensity against slice and determining the background where

the 488nm laser is off. The background is then subtracted via the process >>> math >>> subtract in ImageJ. The raw intensity values are extracted as a one dimensional array of the image using the macros plugin in appendix C. The data file containing intensity values is then converted to a csv file by adding a .csv extension to the file.

For example, if the data file with raw intensity values has the name:"Switching_Test_200.0cycles_exp0.001s_U2OS_rsEGFP2_5mW488_1mW405" a .csv is then appended to the end, and it becomes "Switching_Test_200.0cycles_exp0.001s_U2OS_rsEGFP2_5mW488_1mW405.csv". This csv file is then read using functions in python and parameters that characterize rsEGFP2 are obtained.

4.13 Switch Fatigue Experiment Results

The program in appendix D is used to characterize the switch fatigue for the fluorophores. It uses a double exponential curve fit function in python to provide an exponential fit for the for the extracted mean intensities for odd slices and even slices. The fits are then plotted against the slices to characterize the switch fatigue.

A plot of normalized fluorescence against slices for different 488 nm lasers power are shown in Fig.4-9. Switch fatigue is the ability of rsEGFP2 to survive several switching cycles. The experiments results shown were carried out with U20S cells tagged with rsEGFP 2 for 40 cycles and with 488nm Laser powers of $5\ mW, 10\ mW, 15\ mW and\ 20\ mW$. The percentage of fluorescence(intensity) remaining after a specific slice for the experiments are shown in Table 4-

1,4-2 and 4-3 for experiments on 08/19/2022, 07/19/2022 and 09/23/2022.The intensity were calculated using algorithm in appendix F by making use of the exponential fits parameters obtained in algorithm D. The results in Fig4-9 a,b,c,d and e shows in general a higher switch fatigue resistance but the even slices has better resistance to switch fatigue than the odd slices. The even and odd slices are that for which the value of the slices are even and odd numbers respectively over a range from 0 to 2000 as shown in the plots below. For a given slice there is more fluorescence remaining for the even (red curve) compared to the odd (blue curve) hence a lower switch fatigue in the even compared to the odd.

a

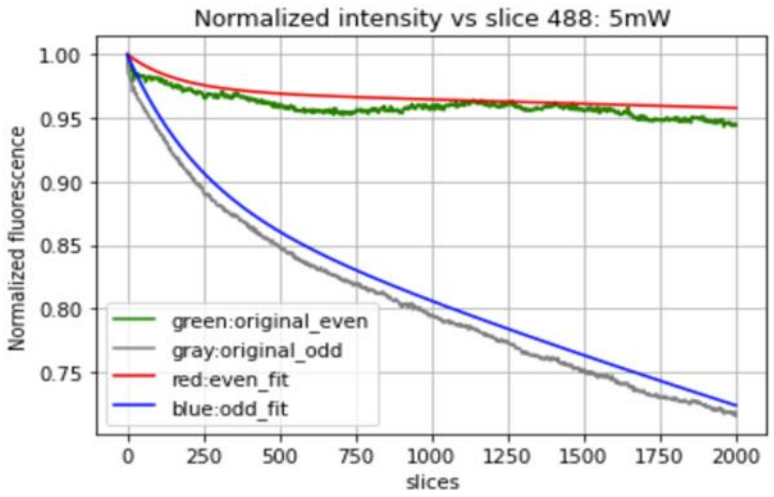

b

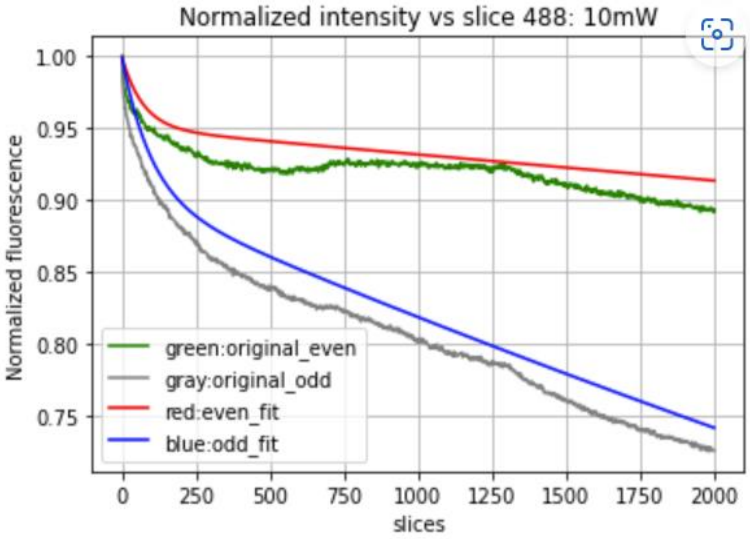
Normalized intensity vs slice 488: 10mW
Normalized fluorescence
slices
green:original_even
gray:original_odd
red:even_fit
blue:odd_fit

c

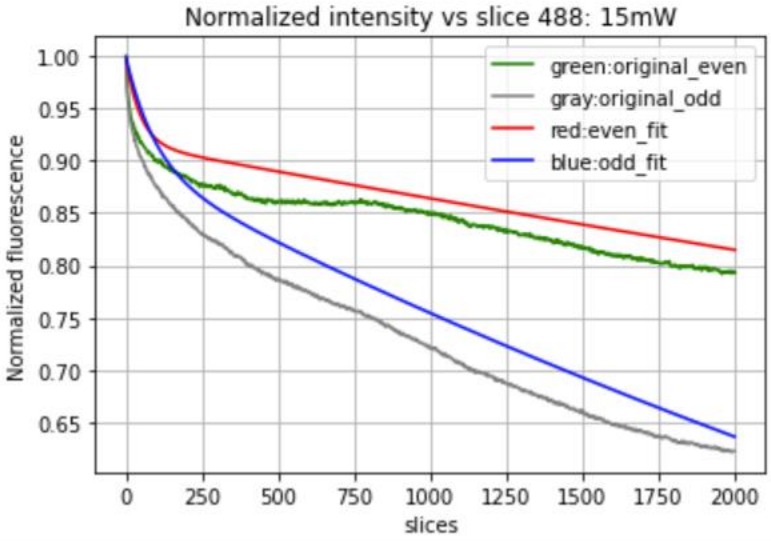
Normalized intensity vs slice 488: 15mW
Normalized fluorescence
slices
green:original_even
gray:original_odd
red:even_fit
blue:odd_fit

d

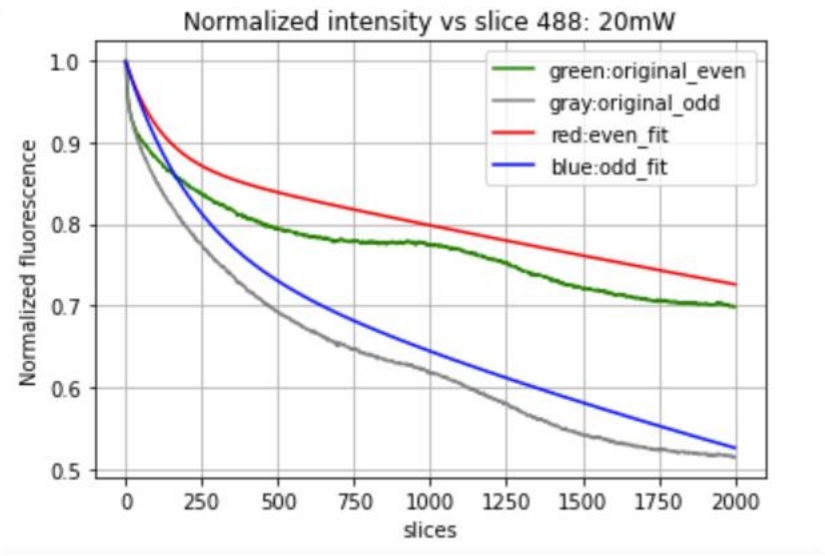

Figure 4-9. A plot of normalized fluorescence for even and odd slices against slices. Activation (even: green: original data), depletion (odd: gray original data), red: fits to even data and blue: fits to odd data curves to characterize the switching fatigues of rsEGFP 2 using 488 nm Laser power of 5 mW, 10 mW, 15 mW and 20 mW for 4-9a,b,c and d respectively. The even slices have better switch fatigue resistance compared to odd. As for example, at 2000 slice around 95%,92%,83% and 74% were remaining for even slices but for odd slice they were 74%,74%,64% and around 53% remaining for the odd slices for the results in Fig.4.9a, b, c and d. Generally, both slices show better switch fatigue resistance attesting to why rsEGFP2 is suitable for non-linear SIM.

Table 4-1. Percentage of intensity remaining at specific slices on 08/19/2022. More switch fatigue at higher laser powers due to tendency to photodamage and higher intensity. Also, the even slices show better switch fatigue resistance compared to the odd.

10mW

Even Intensity remaining (%)	Odd Intensity remaining (%)	Slice
94.1	86.03	500
93.15	81.83	1000
92.24	77.89	1500
91.34	74.13	2000
89.56	67.14	3000

20mW

Even Intensity remaining (%)	Odd Intensity remaining (%)	Slice
83.90	73.03	500
79.83	64.40	1000
76.13	58.11	1500
72.61	52.57	2000
66.04	43.03	3000

15mW

Even Intensity remaining (%)	Odd Intensity remaining (%)	Slice
88.97	82.21	500
86.40	75.43	1000
83.91	69.26	1500
81.48	63.26	2000
76.84	53.61	3000

Table 4-2. Percentage of intensity remaining at specific slices on 07/19/2022. Also, more switch fatigue at higher laser powers due to tendency to photodamage at higher intensity.

20mW

Even Intensity remaining (%)	Odd Intensity remaining (%)	Slice
70.3	67.62	500
55.73	45.73	1000
45.74	30.94	1500
37.89	20.93	2000
26.13	9.59	3000

15mW

Even Intensity remaining (%)	Odd Intensity remaining (%)	Slice
97.7	74.5	500
69.16	58.88	1000
62.87	46.86	1500
57.21	37.32	2000
47.38	23.67	3000

10mW

Even Intensity remaining (%)	Odd Intensity remaining (%)	Slice
76.12	64.24	500
66.34	44.38	1000
58.26	31.94	1500
51.17	23.48	2000
39.49	13.02	3000

Table 4-3. Percentage of intensity remaining at specific slices on 09/23/2022. More switch fatigue at higher laser powers due to tendency to photodamage and higher intensity.

10mW

Even Intensity remaining (%)	Odd Intensity remaining (%)	Slice
94.98	69.23	500
93.94	64.57	1000
93.73	62.46	1500
93.69	60.63	2000
93.67	57.17	3000

20mW

Even Intensity remaining (%)	Odd Intensity remaining (%)	Slice
95.43	74.92	500
94.66	68.03	1000
93.99	63.23	1500
93.33	58.91	2000
92.04	51.16	3000

30mW

Even Intensity remaining (%)	Odd Intensity remaining (%)	Slice
89.04	64.73	500
87.05	58.78	1000
85.85	54.90	1500
84.72	51.38	2000
82.53	45.01	3000

A common trend in the results in Table4-1, Table4-2 and Table4-3 is that with increase in laser power for a given slice the fluorescence (intensity) reduces due to more tendency to photo bleach. The switch fatigue is the tendency of rsEGFP 2 to survive more slices (switch cycles). At $20\ mW$ and with a 1500slices approximately 94%,46% and 76% of maximum intensity (for even intensity) are remaining for the experiment on 09/23/2022,07/19/2022 and 08/19/2022. Clearly, the experiment on 09/23/2022 shows the best switch fatigue because it can survive more slices before permanent photodamage. According to [20] a fluorescent protein has a good switch fatigue if it can survive at least 1100 cycles. To survive at least 1100 cycles then the fluorescence intensity should be decaying at slow rate so that the ratio of fluorescence intensity for a cycle to maximum intensity is high. In this case there is more fluorescence intensity remaining to survive more switch cycles.

Using the results in experiments on 09/23/2022 as an example at 2000slices 93.7%, 93.3% and 84.7% of maximum even intensity is remaining for $10\ mW, 20\ mW\ and\ 30\ mW$ respectively. This agrees with the criteria set by [20] because even at high lasers power there is only a small drop in fluorescence so there is a huge amount remaining for the rsEFGP 2 to switch. Also, the results show that despite a strong switch fatigue resistance in the odd slices(depletion) and even slices(activation), the switch fatigue for the even slice is better in comparison to the odd slice. Taking the results on 09/23/2022 at $30\ mW$ after a given cycle(slice) there is more intensity remaining for the even slice than the odd slice. This is because the even slice is activation, and the odd slice is depletion.

4.14 Time Constant Measurements

The time constants experiments use the arduino code in appendix A to control switching of the lasers and the python code in appendix E to characterize how the properties of the rsEGFP 2 changes with exposure time. The curve fit equation for a given cycle is given in 4-1. For every cycle the time constant (τ) is calculated and it is plotted against the exposure time.

The switching output of the lasers are as shown in Fig.4-2. In a cycle the 405 nm lasers is turned on for exposure time of 1 ms and then turned off and the 488 nm is turned on to read out fluorescence for a longer time. In the next cycle the 405 nm is turned on for 2 ms and the 488 nm is turned on for a longer time again to read out fluorescence and so on until the 20^{th} cycle. So, the power of the 405 nm laser is incremented for every cycle.

4.15 Decay Time Constants vs Exposure Time Results

To measure the decay time constants, I observe the data using the python code to choose an appropriate value for where the 488 nm is initially turning on and to read out fluorescence until the 488 nm is turning off. These points where the 488 nm laser are turning on and turning off are called index start and index stop respectively in the python code in appendix E. These provide a cycle or a slice of the original data. An exponential fit is then done to this slice. An example of this is shown in Fig 4-10a and b where a slice of the original data is taken, and an exponential fit is done for the slice to calculate the decay constants. The original data is shown as blue dots, and the exponential fits is a red line. Figure 4-11 shows the graphical trend from

plotting the time constants against the exposure time from the characterized raw data. The graphs were obtained by using the python code in appendix E. The experiments were for 40 cycles.

The quality of fitness of the curve depends on the raw data characterized and the values chosen for the index stop and index start shown in the python code. The experiments were done for different powers of the 405 nm laser, and the power meter shown in Fig.4-7 is used to measure corresponding power of the 488 nm laser. The power values of the lasers are shown top on the curve. Also, the trends show two things: In one case the decay time constants approximately increase with the exposure time for low exposures and saturate at high exposures and in other cases is changing over a small range and with an average of around 1ms for higher powers exposures (15 mW,20 mW and 25 mW) and around 4 ms for lower powers (at 5 mW).This indicates that rsEGFP 2 switches faster at long exposures.

a

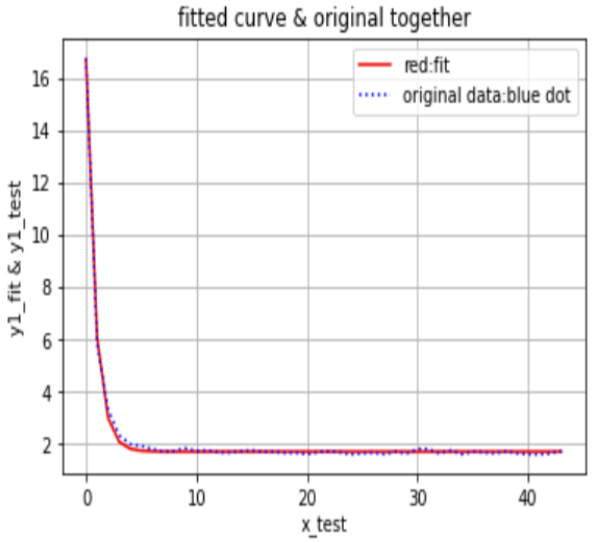

b

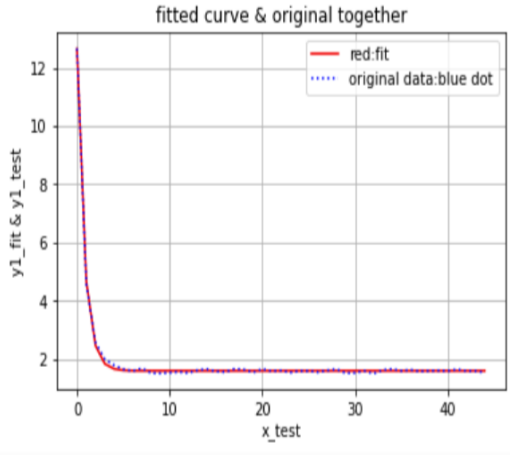

Figure 4-10. Fitted curves and original data. a and b are fitted curves (red) for a slice (a cycle) of the original data.

a

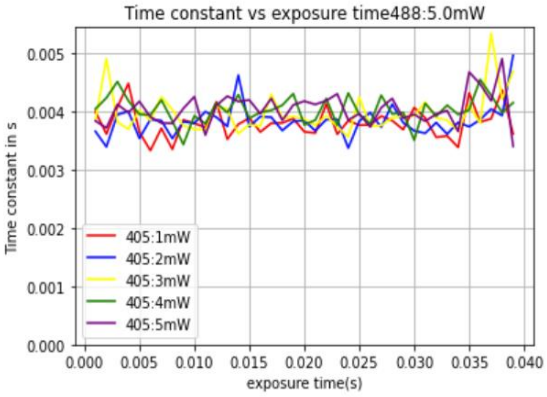

b

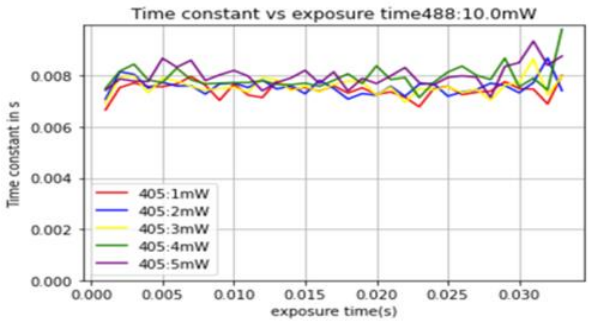

c

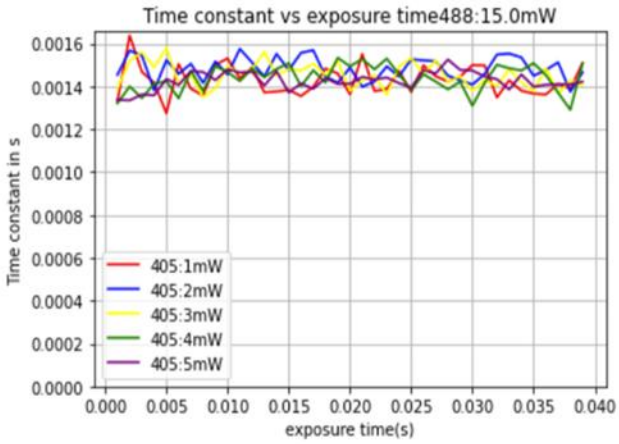

d

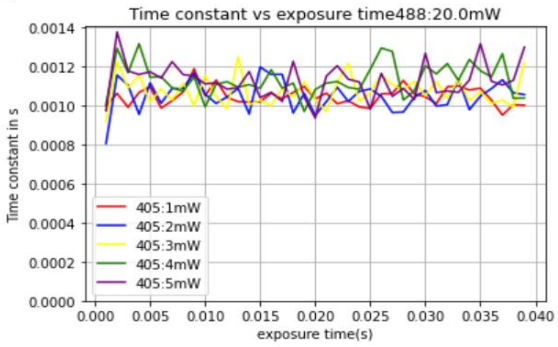

e

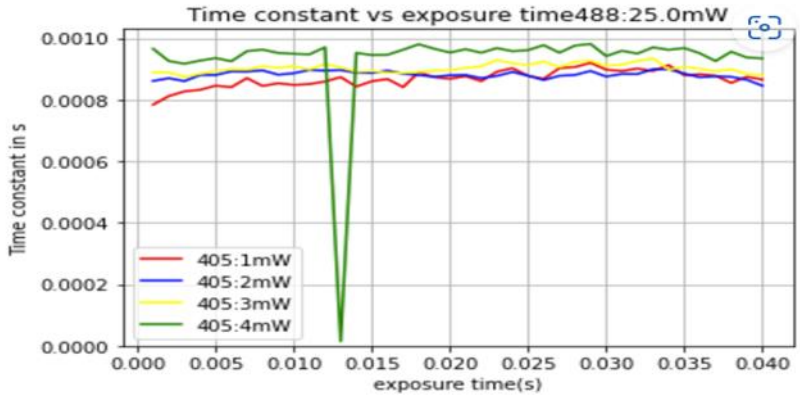

Figure 4-11. Decay Time constant versus exposure time curve for rsEGFP 2.a, c,d e, Approximate trends shows the time constant changes over a small range.b,d The time constants increase by a small range for small exposures and saturates at high exposures. The experiments were for 40 cycles and powers of 405 nm lasers were 1 mW,2 mW,3 mw,4 mW and 5 mW. The powers of 488 nm lasers were 5 nm,10 nm, 15 nm,20 nm and 25 nm.

4.16 Peak Intensity Versus Exposure Time Results

Figure 4-12 shows the graph trends of the peak intensity against the exposure time of the 405 nm laser for different powers of the 405 nm and 488 nm Lasers. An increase in the 405 nm laser power or the 405 nm exposure time provides more activation of the fluorophore. The experiments were for 40 cycles. The peak intensity (highest point of the 488 nm laser pulse) is plotted against the exposure times of the camera. The minimum exposure time is $1\ ms$. The plot shows that the intensity increases with the exposure time for low exposure times and saturates at high exposure time confirming the suitability of rsEGFP 2 for non-linear SIM. The activation time constant increases as the 405 nm laser power increases for a given 488 nm laser power. In Fig.4-12 for the 488 nm power of 5 mW the average activation time constant for the fits was 0.01 s and 7.9 ms when the 405 nm laser power is 1 mW and 5 mW respectively. Also, for a set of powers of 405 nm (1 mW, 2 mW, 3 mW, 4 mW,5 mW) the average time constant increases with decrease in 488 nm laser power. For example, the average time constant was 9 ms and 4 ms at 5 mW and 25 mW 488 lasers power respectively.

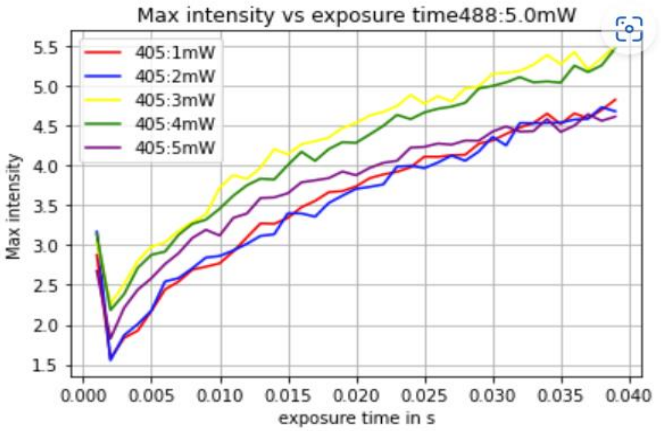
Max intensity vs exposure time488:5.0mW
405:1mW
405:2mW
405:3mW
405:4mW
405:5mW
Max intensity
exposure time in s

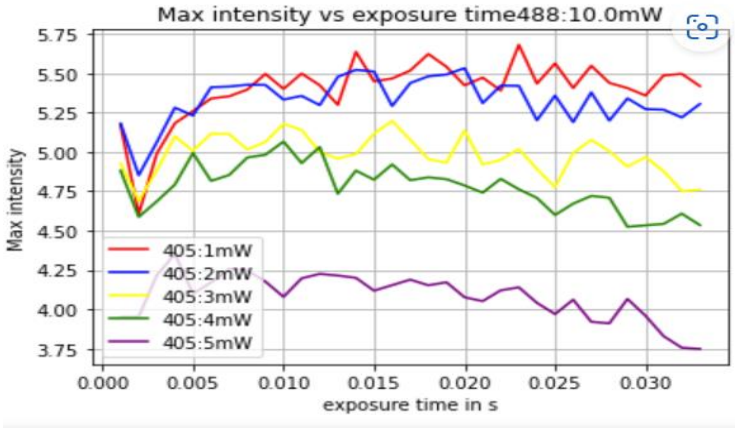
Max intensity vs exposure time488:10.0mW
405:1mW
405:2mW
405:3mW
405:4mW
405:5mW
Max intensity
exposure time in s

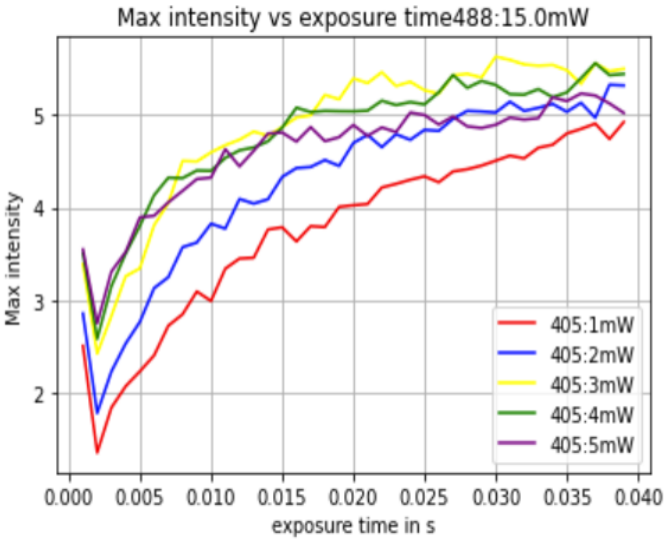
Max intensity vs exposure time488:15.0mW
405:1mW
405:2mW
405:3mW
405:4mW
405:5mW
Max intensity
exposure time in s

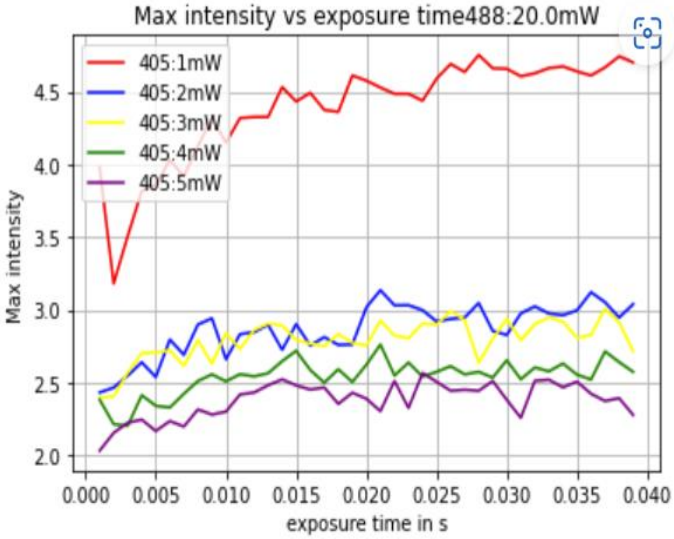
Max intensity vs exposure time488:20.0mW
405:1mW
405:2mW
405:3mW
405:4mW
405:5mW
Max intensity
exposure time in s

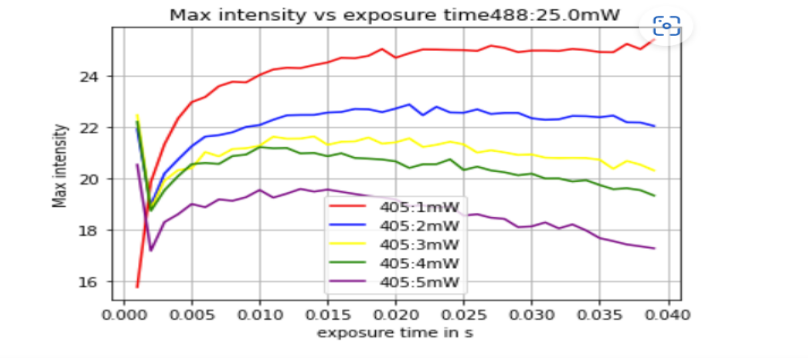

Figure 4-12. Peak intensity versus exposure time curve for rsEGFP 2. Approximate trend shows the peak intensity increases with exposure time and saturates at higher exposure time. The experiments were for 40 cycles and different powers of 405 nm Lasers and 488 nm Lasers. The powers of the 405 nm Lasers were 1 mW,2 mW,3 mW,4 mW and 5 mW. The power of the 488 nm lasers were 5 mW,10 mW, 15 mW,20 mW and 25 mW.

4.17 Background versus Exposure Time Results

The background (B) in the algorithm in appendix E was plotted against the exposure time for each cycle to indicate how it is varying with exposure time. For well fitted curves, the background is approximately decreasing or increasing with exposure time. Figure 4-13 shows the results of the plot of background against exposure times for 40 cycles. The plots show that the background is approximately decreasing as exposures increases. Figure 4-13a, b,c and e show a rise in the background versus exposure times while Figure 4-13d shows an approximate drop. In all experiments, the background changes at a small amount with average of approximately 2 at low power (5 mW) and a maximum value of around 7 at high power (20 mW). This shows a nice property of rsEGFP 2 for nonlinear SIM. A drop in background means more fluorescence and a small rise means fluorescence is reducing at a small amount. Also, the average background is a bit more at high powers compared with low powers.

a

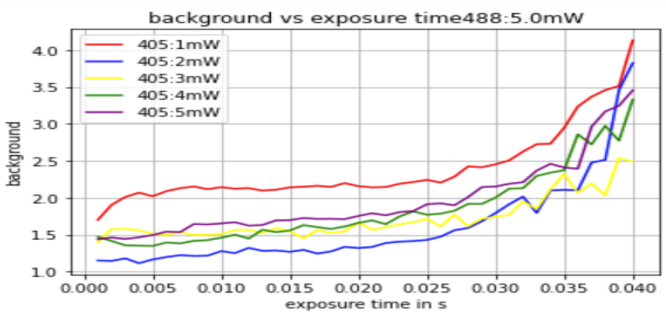
background vs exposure time488:5.0mW
405:1mW
405:2mW
405:3mW
405:4mW
405:5mW
background
exposure time in s

b

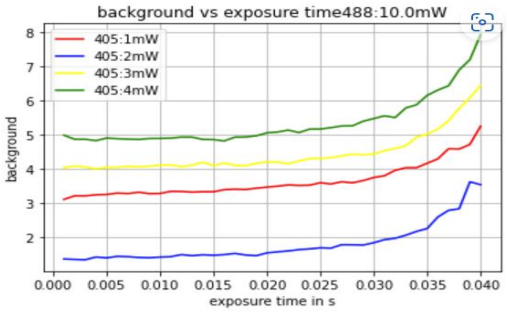
background vs exposure time488:10.0mW
405:1mW
405:2mW
405:3mW
405:4mW
background
exposure time in s

c

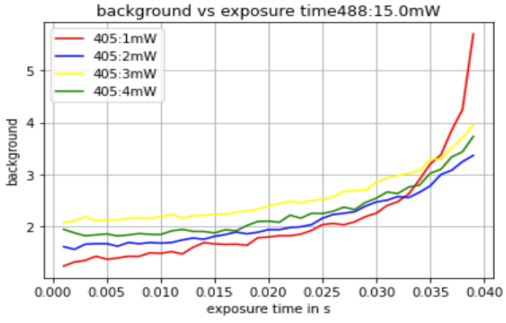
background vs exposure time488:15.0mW
405:1mW
405:2mW
405:3mW
405:4mW
background
exposure time in s

d

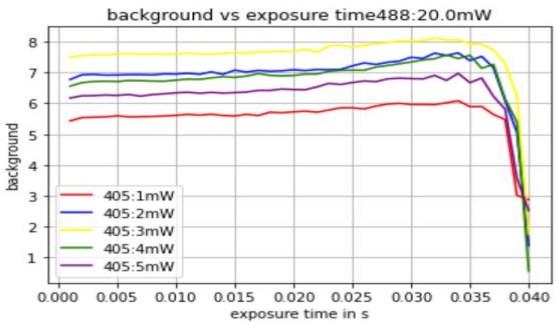
background vs exposure time488:20.0mW
405:1mW
405:2mW
405:3mW
405:4mW
405:5mW
background
exposure time in s

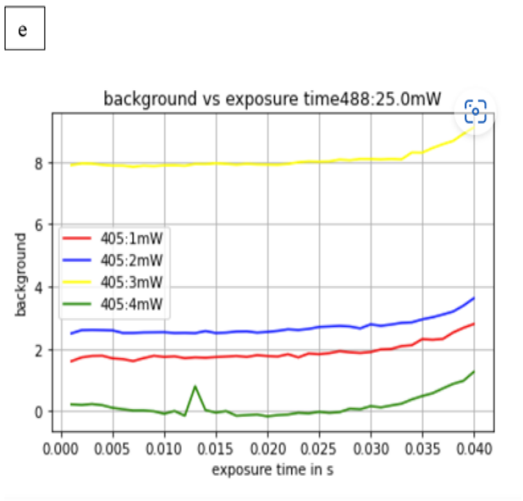

Figure 4-13. Background versus exposure time curve for rsEGFP 2. Approximate trend shows the background increasing or decreasing with exposure time. a,b,c and e show a rise with exposure time while b show an approximate drop. The background changes by a small amount with average of around 2 at low powers. The experiments were for 40 cycles and different powers of 405 nm Lasers and 488 nm Lasers. The powers of the 405 nm Lasers were 1 mW,2 mW,3 mW,4 mW and 5 mW. The power of the 488 nm lasers were 5 mW,10 mW, 15 mW,20 mW and 25 mW.

4.18 Ratio of Background to Maximum Intensity Results

Algorithm in appendix E also calculates the ratio of background to maximum intensity (B/A+B) for each cycle. A plot of the ratio of background to maximum intensity is shown in Figure 4-14 for 40 cycles.Fig.4-14a, b,c,d and e shows an approximate drop in the ratio of background to maximum intensity as exposure times increases. The drop is over a small range and with an average value of around 0.1 at low powers (5 mW) and approximately 0.189 at high powers(20 mW). The experiments were for different 488 laser powers of 5 mW,10 mW,15 mW,20 mW and 25 mW. The 405 laser powers were 1 mW,2 mW,3 mW,4 mW and 5 wW.The

small average value for the background to maximum intensity attest to why rsEGFP 2 is suitable for non-linear SIM.

a

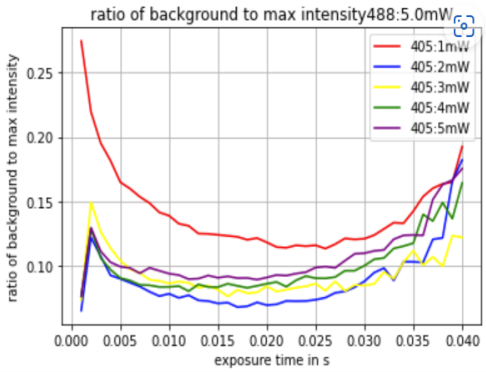

b

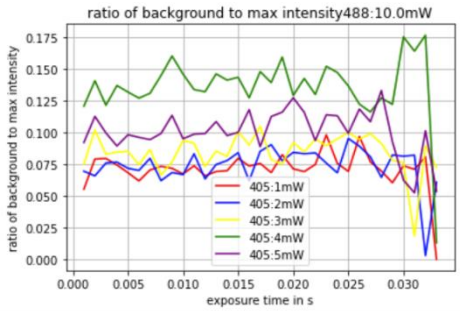

c

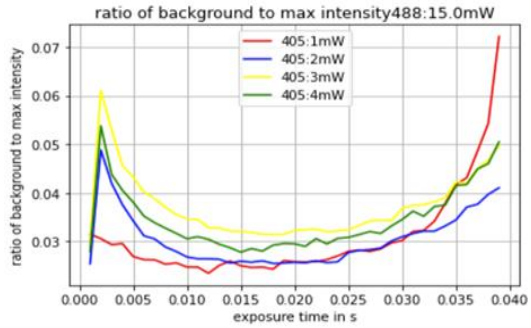

d

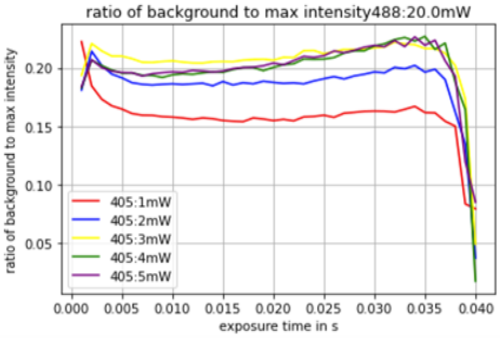

e

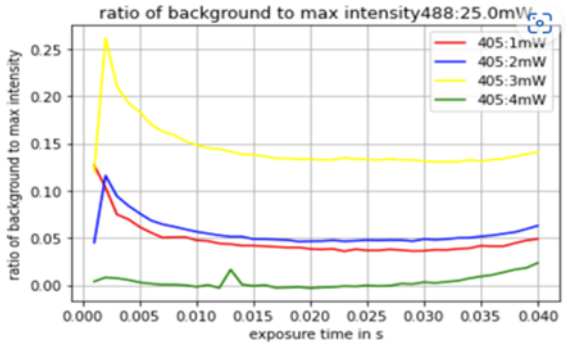

Figure 4-14. Plots of ratio of background to maximum intensity versus exposure for different lasers powers. a,b,c,d,e show that the ratio is approximately inversely proportional to the exposures attesting to why rsEGFP 2 is suitable for non-linear SIM.

4.19 Comparison of my results to previous results using rsEGFP2

Grotjohann et al. [18] characterized rsEGFP2 using switch fatigue and deactivation (off switching times) behavior using RESOLFT (Reversible Saturable Optical Linear Fluorescence Transitions). Fig. 1-6 [18] in chapter one compared the switch cycles of rsEGFP to rsEGFP2. These switch results were also presented in table1-4 [18] and it is clearly seen that rsEGFP2 has lower switch fatigues since it can survive well over 1100 cycles before photobleaching. This is like the switching results obtained in Fig.4-9 as rsEGFP2 can switch well over 1100 image frames. Also, the off-rate characteristics of rsEGFP 2 is shown in Fig. 4-15[18] below. At approximately 9 $KWcm^{-2}$ the off-switching halftime (time to deactivate rsEGFP 2 to 50% of fluorescence) is approximately $2.5\ ms$. It is also clear that as the deactivation

illumination(491nm) power increases the off-switching times becomes faster(reduces). This is also like the deactivation time constants results shown in Fig.4-7. The average decay time constants were 1 ms for higher illumination (488 nm lasers of 15 mW, 20 mW and 25 mW) and 4 ms for lower 488 nm illumination (5 mW). Which shows that in both results rsEGFP2 switches faster at long exposures.

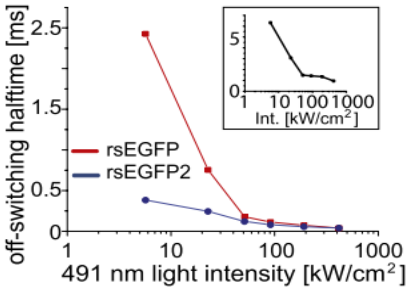

Figure 4-15 [18]. Comparison of off switching behavior of rsEGFP and rsEGFP2. At low illumination rsEGFP2 switches slower compared to rsEGFP . At high illumination (above 100 $KWcm^{-2}$) there is no difference in switching times. Inset graph shows the ratio of the off-switching halftime of rsEGFP divided by the off-switching halftime of rsEGFP2 against the 491 nm light.

4.20 Shortcomings of the Experiments

It was difficult to provide a correct fit at high powers of 488 nm Laser because the fluorescence is decaying at a fast rate. A typical example is shown in Fig.4-16 for the experiment on 11/11/2022 on U20S cells tagged with rsEGFP 2 at 488 nm laser power of 40 mW and 405 nm laser power of 2 mW for 20 cycles. Fig. 4-17 shows the first cycle. The fluorescence is decaying very fast as seen with mostly straight lines. Consequently, it was difficult for the curve fit function in python to provide an exponential fit.

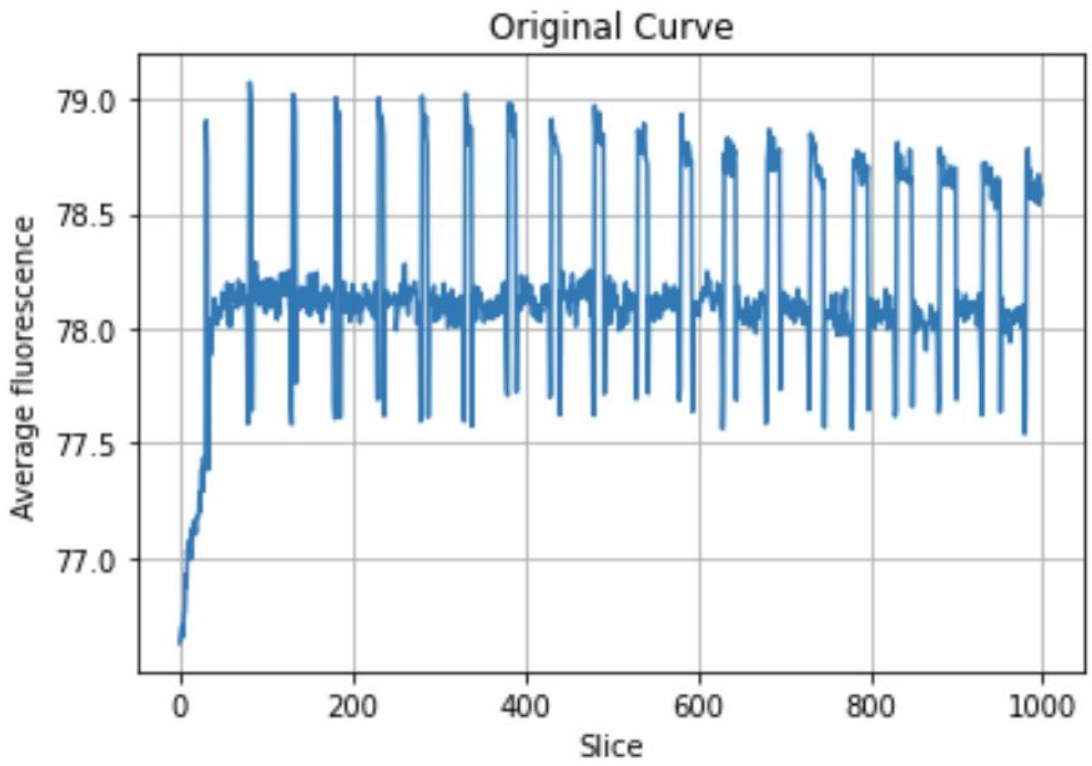

Figure 4-16. Graph of fluorescence against slice for 20 cycles. A read out 488 nm laser power of 40 mW makes fluorescence to drop quickly. The 405 nm laser power of 2 mW was used.

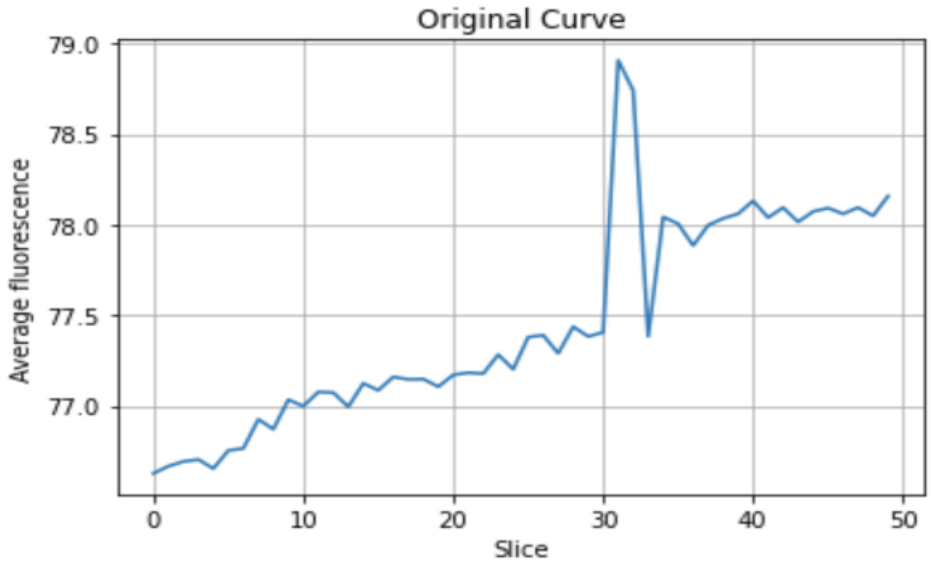

Figure 4-17. Zooming in on a section of the slice to explain shortcomings. The fluorescence is seen decaying faster with mostly straight lines.

Chapter Five

Summary of Results and Further Recommendations

5.1 Conclusion and recommendations

The work in this thesis characterized rsEFFP 2 (reversible photo switchable Enhanced Green Fluorescent Protein 2) to determine its suitability for non-linear Structural Illumination Microscopy. Statistical parameters such as switch fatigue, time constant (decay constants) and ratio of background to maximum intensity were observed with increasing exposure times (as presented in chapter four) to characterize rsEGFP 2. To determine these parameters raw data were taken using steps one to steps eight (explained in chapter four) and the algorithms in appendix C, D, E and F are used to calculate the parameters. Results shows that rsEGFP 2 can survive large switch cycles (≥1100) and the background to maximum intensity is also approximately changing at a very small amount with increase in exposure times. Backgrounds with an average of 2 at low powers (5 mW) and background to maximum intensity of around 0.1 was obtained at low powers (5 mW). Also, the time constant of around 1 ms at high laser powers of 20 mW and approx. 4 ms at low laser powers (5 mW) was obtained. The time constant also increase with exposure at low exposures and saturates at high exposures confirming the right behavior of rsEGFP 2 and its suitability for non-linear SIM (Structured Illumination Microscopy). Recommendations for further works are stated below.

- We need to characterize red rsFPs (reversible photo switchable Fluorescent Proteins) to determine their suitability for SIM (Structured Illumination Microscopy). Red rsFPs

emits red with green-orange light. Because of the longer wavelength of green light compared to violet light (used to turn on rsEGFP 2) , red rsFPs provide more photostability than green emitting rsEGFP 2 which limits their use in multicolor imaging. Francesca Pennacchietti et al. [20] characterized red shifting rsFPs called rsFusionRed to confirm their suitability for live cell RESOLFT nanoscopy.

- We need to characterize rsEGFP 2 for high-speed multicolor SIM. Taylor Hinsdale et al.[32] confirms that by using hexagonal single mode fiber array as opposed to using gratings or programmable devices such as spatial light modulation to generate structured light patterns image frames can be acquired at a high speed in the region of 100 SIM frames per second. SIM set ups that uses diffraction elements like gratings are only limited to speed of the order of 1 Hz for full SIM acquisitions.
- We need to characterize the autofluorescence of the sample. Autofluorescence means U2OS cells without labelling with fluorescent proteins.
- We need to use rsEGFP 2 in non-linear Structured Illumination Microscopy to determine resolution for different biological samples.

REFERENCES

[1] R. S. Westfall, "Science and patronage: Galileo and the telescope," *Isis,* vol. 76, no. 1, pp. 11-30, 1985.

[2] D. B. Murphy, *Fundamentals of light microscopy and electronic imaging*. John Wiley & Sons, 2002.

[3] N. Chaffey, "Alberts, B., Johnson, A., Lewis, J., Raff, M., Roberts, K. and Walter, P. Molecular biology of the cell. 4th edn," ed: Oxford University Press, 2003.

[4] F. W. Rost, *Fluorescence microscopy*. Cambridge University Press, 1992.

[5] E. Instruments. "What is the Difference between Luminescence, Photoluminescence, Fluorescence, and Phosphorescence?" https://www.edinst.com/blog/photoluminescence-differences/ (accessed.

[6] B. Valeur and M. N. Berberan-Santos, *Molecular fluorescence: principles and applications*. John Wiley & Sons, 2012.

[7] J. R. Lakowicz, *Principles of fluorescence spectroscopy*. Springer, 2006.

[8] D. E. Wolf, "Fundamentals of fluorescence and fluorescence microscopy," in *Methods in cell biology*, vol. 114: Elsevier, 2013, pp. 69-97.

[9] R. Heintzmann, T. M. Jovin, and C. Cremer, "Saturated patterned excitation microscopy—a concept for optical resolution improvement," *JOSA A,* vol. 19, no. 8, pp. 1599-1609, 2002.

[10] R. Lin, "Super-Resolution Structured Illumination Microscopy with Adaptive Optics," Ph.D., University of Georgia, United States -- Georgia, 28775696, 2021. [Online]. Available: https://www.proquest.com/dissertations-theses/super-resolution-structured-illumination/docview/2623933751/se-2?accountid=14537

https://galileo-uga.primo.exlibrisgroup.com/openurl/01GALI_UGA/01GALI_UGA:UGA?url_ver=Z39.88-2004&rft_val_fmt=info:ofi/fmt:kev:mtx:dissertation&genre=dissertations&sid=ProQ:ProQuest+Dissertations+%26+Theses+Global&atitle=&title=Super-Resolution+Structured+Illumination+Microscopy+with+Adaptive+Optics&issn=&date=2021-01-01&volume=&issue=&spage=&au=Lin%2C+Ruizhe&isbn=9798780616658&jtitle=&btitle=&rft_id=info:eric/&rft_id=info:doi/

[11] T. J. Chozinski, L. A. Gagnon, and J. C. Vaughan, "Twinkle, twinkle little star: Photoswitchable fluorophores for super-resolution imaging," *FEBS letters,* vol. 588, no. 19, pp. 3603-3612, 2014.

[12] J. E. Fitzgerald, J. Lu, and M. J. Schnitzer, "Estimation theoretic measure of resolution for stochastic localization microscopy," *Physical review letters,* vol. 109, no. 4, p. 048102, 2012.

[13] J. Ries, C. Kaplan, E. Platonova, H. Eghlidi, and H. Ewers, "A simple, versatile method for GFP-based super-resolution microscopy via nanobodies," *Nature methods,* vol. 9, no. 6, pp. 582-584, 2012.

[14] F. Opazo *et al.*, "Aptamers as potential tools for super-resolution microscopy," *Nature methods,* vol. 9, no. 10, pp. 938-939, 2012.

[15] H. Deschout *et al.*, "Precisely and accurately localizing single emitters in fluorescence microscopy," *Nature methods,* vol. 11, no. 3, pp. 253-266, 2014.
[16] U. Rothbauer *et al.*, "Targeting and tracing antigens in live cells with fluorescent nanobodies," *Nature methods,* vol. 3, no. 11, pp. 887-889, 2006.
[17] D. M. Shcherbakova, P. Sengupta, J. Lippincott-Schwartz, and V. V. Verkhusha, "Photocontrollable fluorescent proteins for superresolution imaging," *Annual review of biophysics,* vol. 43, pp. 303-329, 2014.
[18] T. Grotjohann *et al.*, "rsEGFP2 enables fast RESOLFT nanoscopy of living cells," *Elife,* vol. 1, p. e00248, 2012.
[19] S. W. Hell and J. Wichmann, "Breaking the diffraction resolution limit by stimulated emission: stimulated-emission-depletion fluorescence microscopy," *Optics letters,* vol. 19, no. 11, pp. 780-782, 1994.
[20] F. Pennacchietti *et al.*, "Fast reversibly photoswitching red fluorescent proteins for live-cell RESOLFT nanoscopy," *Nature methods,* vol. 15, no. 8, pp. 601-604, 2018.
[21] E. H. Rego *et al.*, "Nonlinear structured-illumination microscopy with a photoswitchable protein reveals cellular structures at 50-nm resolution," *Proceedings of the National Academy of Sciences,* vol. 109, no. 3, pp. E135-E143, 2012.
[22] T. Grotjohann *et al.*, "Diffraction-unlimited all-optical imaging and writing with a photochromic GFP," *Nature,* vol. 478, no. 7368, pp. 204-208, 2011.
[23] M. Hofmann, C. Eggeling, S. Jakobs, and S. W. Hell, "Breaking the diffraction barrier in fluorescence microscopy at low light intensities by using reversibly photoswitchable proteins," *Proceedings of the National Academy of Sciences,* vol. 102, no. 49, pp. 17565-17569, 2005.
[24] M. Chalfie, Y. Tu, G. Euskirchen, W. W. Ward, and D. C. Prasher, "Green fluorescent protein as a marker for gene expression," *Science,* vol. 263, no. 5148, pp. 802-805, 1994.
[25] P. Bethge, R. Chéreau, E. Avignone, G. Marsicano, and U. V. Nägerl, "Two-photon excitation STED microscopy in two colors in acute brain slices," *Biophysical journal,* vol. 104, no. 4, pp. 778-785, 2013.
[26] G. T. Dempsey, J. C. Vaughan, K. H. Chen, M. Bates, and X. Zhuang, "Evaluation of fluorophores for optimal performance in localization-based super-resolution imaging," *Nature methods,* vol. 8, no. 12, pp. 1027-1036, 2011.
[27] M. J. Rust, M. Bates, and X. Zhuang, "Sub-diffraction-limit imaging by stochastic optical reconstruction microscopy (STORM)," *Nature methods,* vol. 3, no. 10, pp. 793-796, 2006.
[28] T. J. Gould, V. V. Verkhusha, and S. T. Hess, "Imaging biological structures with fluorescence photoactivation localization microscopy," *Nature protocols,* vol. 4, no. 3, pp. 291-308, 2009.
[29] M. G. Gustafsson, "Surpassing the lateral resolution limit by a factor of two using structured illumination microscopy," *Journal of microscopy,* vol. 198, no. 2, pp. 82-87, 2000.
[30] M. G. Gustafsson *et al.*, "Three-dimensional resolution doubling in wide-field fluorescence microscopy by structured illumination," *Biophysical journal,* vol. 94, no. 12, pp. 4957-4970, 2008.
[31] M. G. Gustafsson, "Nonlinear structured-illumination microscopy: wide-field fluorescence imaging with theoretically unlimited resolution," *Proceedings of the National Academy of Sciences,* vol. 102, no. 37, pp. 13081-13086, 2005.
[32] T. A. Hinsdale, S. Stallinga, and B. Rieger, "High-speed multicolor structured illumination microscopy using a hexagonal single mode fiber array," *Biomedical Optics Express,* vol. 12, no. 2, pp. 1181-1194, 2021.

APPENDICES

A. Arduino code that controls switching of the laser

```
const int LASER_488= 13; //" LASER_488 is a LASER LED connected to digital pin 13 on
Arduino"
const int TRIGGER=12;//" TRIGGER is a LASER LED connected to digital pin 12 on Arduino"
const int LASER_405=11;//" LASER_405 is a LASER LED connected to digital pin 11 on
Arduino"
volatile int laser_state=0;
volatile int count = 0; // keep track of camera exposures
volatile int start_405 = 2;
volatile int stop_405 = 3;
volatile int cycle = 50;
String incoming;
void setup() {
  Serial.begin(9600); // opens the serial port at 9600bits per second
  Serial.println("Starting"); // print starting at the serial port buffer
  pinMode(LASER_488,OUTPUT); // sets LASER_488 as an output
  pinMode(TRIGGER,INPUT);   // sets TRIGGER as output
  pinMode(LASER_405,OUTPUT);  // sets LASER_405 as output
 attachInterrupt(digitalPinToInterrupt(TRIGGER),change,CHANGE);
```

```
  digitalWrite(LASER_488,LOW);
  digitalWrite(LASER_405,LOW);
  }

void loop(){
  if (Serial.available()>0)
  {
  stop_405++;

  //incoming = "R";
  incoming = Serial.readString();
  if  (incoming=="R"){
    Serial.println("soft reset");
    stop_405=3;
    digitalWrite(LASER_488,LOW);
    digitalWrite(LASER_405,LOW);
  }
}}

void change() {
  if (digitalRead(TRIGGER)==HIGH){
    count++;
```

```
//Serial.println(count);
if (count == cycle) {
  count = 0;
  stop_405 = stop_405 + 1;
        }
if (stop_405==cycle){
  stop_405 = 3;
 }

if (count>=start_405 && count<stop_405) {
  //Serial.println("405 high");
  digitalWrite(LASER_405, HIGH);
  laser_state = 1;
        }
if (count == stop_405) {
  //Serial.println("488 high");
  digitalWrite(LASER_488, HIGH);
}
if (count == (cycle-1)) {
  //Serial.println("488 low");
  digitalWrite(LASER_488, LOW);
}
```

```
  } else {
    //Serial.println("off");
    if (laser_state==1) {
      digitalWrite(LASER_405,LOW);
      laser_state=0;
    }
    }
}
```

B. Python code use to set the frame rate and exposure times of the camera

```
datapath = r'C:/Users/Public/Documents/data'
basepath = r'C:/Users/Public/Documents/python_code/sim_sona_p38'
camerapath = r'C:\Users\Public\Documents\python_code\AndorSONA\andorsona_scmos'

import os,sys,time
import tifffile as tf
from pylab import imshow
try:
   sys.path.index(camerapath)
except:
   sys.path.append(camerapath)
import numpy as np

import andor_sona_p36 as sona
import os,sys,time

def test_one(nimgs = 1000):
   # initialize data
   cam = sona.scmos()
   exposure_time=0.001
   cam.set_exposure_time(exposure_time) #seconds
```

```
    cam.set_trigger_mode(0) # internal
    cam.set_aoi_layout(0)
    cam.set_cycle_mode(1)
    cam.set_gain_mode(1)
    cam.set_aoi_binning(0)
    cam.get_camera_temperature()
    cam.set_aoi(868, 910,64,64)
    nx,ny = cam.get_aoi_size()
    cam.set_frame_rate(500)
    data = np.zeros((nimgs,nx,ny), dtype=np.int16)
    # take data
    cam_start_time = time.time()
    cam.queue_buffer()
    cam.start_acquisition()
    frame_times=[]
    for m in range(nimgs):
        start_time = time.time()
        cam.wait_buffer()
        data[m] = cam.get_img()
        cam.queue_buffer()
        #r = sona.at64.AT_QueueBuffer(cam.Handle, sona.ct.cast(cam.buffer.ctypes.data,
sona.AT_U8) ,cam.BufferSize)
        end_time = time.time()
```

```
        frame_time=end_time-start_time
        frame_times.append(frame_time)
        print('frame time: [11]m'.format(tt=(end_time-start_time)))
    cam.stop_acquisition()
    cam.flush_buffer()
    cam_end_time = time.time()
    frame_times=np.array(frame_times)
    print('Total time: [11]'.format(tt=(cam_end_time-cam_start_time)))
    read_out_time=cam.get_readout_time()
    print("read out time:",read_out_time)
    print("Maximum frame rate:", 1/(exposure_time+read_out_time))
    print("Mean:",np.mean(frame_times))
    print("frame rate for a frame:",1/np.mean(frame_times))
    print("standard deviation:",np.std(frame_times))
    print("Interface transfer rate:",cam.get_max_interface_transfer_rate())
    cam.close_camera()
    tf.imsave('Switching_Test_' + str(nimgs/10) + 'cycles_exp' +
str(exposure_time)+'s_U2OS_rsEGFP2_25mW488_5mW405_cell5.tif',data)
    return data
```

C. Macros algorithm to extract raw values from switch cycles.

```
// Measure Stack
//
// This macro measure all the slices in a stack.

  macro "Measure Stack" {
       saveSettings;
       setOption("Stack position", true);
       for (n=1; n<=nSlices; n++) {
          setSlice(n);
          run("Measure");
       }
      restoreSettings;
  }
```

D. Python codes to obtain a nice fit for the fluorescence.

```
Laser_488_power=int( input("Laser_488_power:  "))
```

```
import pandas as pd
from scipy.optimize import curve_fit
import matplotlib.pyplot as plt
import numpy as np
import warnings
warnings.filterwarnings("ignore")
#y=mean
#x=slices
df=pd.read_csv("20220819-171152_cycle_U2OS_rsEGFP2_nb_nsim20_20mW_.csv")
y1=[] #a list to hold all means for even slices
def fun1(df):
    for i,row in df.iterrows():
        if (i+1)%2==0:
            y1.append(row["Mean"])
    return y1
y1=fun1(df)
y1=np.array(y1)
y2=[] #a list to hold all means for odd slices
def fun2(df):
    for i,row in df.iterrows():
        if (i+1)%2!=0:
            y2.append(row["Mean"])
    return y2
```

```
y2=fun2(df)
y2=np.array(y2)
x1=[] #to hold all the even slices
def fun3(df):
    for i,row in df.iterrows():
        if (i+1)%2==0:
            x1.append(row["Slice"])
    return x1
x1=fun3(df)
x1=np.array(x1)
x2=[] #to hold all odd slices
def fun4(df):
    for i,row in df.iterrows():
        if (i+1)%2!=0:
            x2.append(row["Slice"])
    return x2
x2=fun4(df)
x2=np.array(x2)
print("Statistical measure for even means vs even slices")
def exponential_model(x1,a,A,b,B):
    y1=A*np.exp(-a*x1)+B*np.exp(-b*x1) # paratemeter(beta)=(a,A,b,B)
    return y1
popt,pcov=curve_fit(exponential_model,x1,y1)
```

```
a,A,b,B=popt
C=1/(A+B)
print("Optimized parameters")
print("a:",a)
print("A:",A)
print("b:",b)
print("B:",B)
print("To test how the model fits the actual data for even mean")
y1_model=exponential_model(x1,a,A,b,B)
y1_model_normalized=C*exponential_model(x1,a,A,b,B)
plt.scatter(x1,y1)
plt.plot(x1,y1_model,color='r')
plt.xlabel(" even slices")
plt.ylabel(" even Mean")
plt.title("graph of even mean vs even slices")
plt.show()
print("To estimate covariance effect")
plt.imshow(np.log(np.abs(pcov)))
plt.colorbar()
plt.show()
print("Errors in the optimized parameters")
error=np.sqrt(np.diag(pcov))
error_a,error_A,error_b,error_B=error
```

```
print("error_a:",error_a)

print("error_A:",error_A)

print("error_b:",error_b)

print("error_B:",error_B)

#residuals for even means

residuals=y1-y1_model

print("residual statistical values for for even mean")

mean=np.mean(residuals)

maxim=np.max(residuals)

minim=np.min(residuals)

sd=np.std(residuals)

print("mean:",mean)

print("maximum:",maxim)

print("minimum:",minim)

print("standard deviation:",sd)

plt.plot(residuals,color="navy")

plt.xlabel('slices')

plt.ylabel("residual")

plt.title("The graph of even mean residuals")

plt.grid(True)

plt.show()

#correlation of actual vs model for even means

corr1=np.corrcoef(y1, y1_model)
```

```
print("correlation of y1:",corr1)
print("Statistical measure for odd means vs odd slices")
def exponential_model(x2,a,A,b,B):
    y2=A*np.exp(-a*x2)+B*np.exp(-b*x2) # paratemeter(beta)=(a,A,b,B)
    return y2
popt,pcov=curve_fit(exponential_model,x2,y2)
a,A,b,B=popt
D=1/(A+B)
print("Optimized parameters")
print("a:",a)
print("A:",A)
print("b:",b)
print("B:",B)
print("To test how the model fits the actual data")
y2_model=exponential_model(x2,a,A,b,B)
y2_model_normalized=D*exponential_model(x2,a,A,b,B)
plt.scatter(x2,y2)
plt.plot(x2,y2_model,color='r')
plt.xlabel(" odd slices")
plt.ylabel(" odd Mean")
plt.title("graph of  odd mean vs odd slices")
plt.show()
print("To estimate covariance effect")
```

```
plt.imshow(np.log(np.abs(pcov)))
plt.colorbar()
plt.show()
print("Errors in the optimized parameters")
error=np.sqrt(np.diag(pcov))
error_a,error_A,error_b,error_B=error
print("error_a:",error_a)
print("error_A:",error_A)
print("error_b:",error_b)
print("error_B:",error_B)
#residuals for odd means
residuals=y2-y2_model
print("residual statistical values for odd mean")
mean=np.mean(residuals)
maxim=np.max(residuals)
minim=np.min(residuals)
sd=np.std(residuals)
print("mean:",mean)
print("maximum:",maxim)
print("minimum:",minim)
print("standard deviation:",sd)
plt.plot(residuals,color="navy")
plt.xlabel('slices')
```

```
plt.ylabel("residual")

plt.title("The graph of odd mean residuals")

plt.grid(True)

plt.show()

#correlation of actual vs model for odd means

corr2=np.corrcoef(y2, y2_model)

print("correlation of y2:",corr2)

plt.plot(x1,y1_model_normalized,'r',x2,y2_model_normalized,'b')

plt.legend(["red:even","blue:odd"])

plt.grid(True)

plt.xlabel("slices")

plt.ylabel("Normalized Y1 & Y2 even & odd")

plt.title("Even and odd intensity vs slice "  + "488: "+str(Laser_488_power)+"mW")

plt.show()
```

E. Python codes to calculate the time constants, background, and the ratio of background to maximum intensity.

```
import pandas as pd

from scipy.optimize import curve_fit

import numpy as np

import matplotlib.pyplot as plt

import warnings

warnings.filterwarnings("ignore")
```

```
#y=mean
#x=slice
exposure_time=float(input("Laser_405 exposure time:  ")) #in milliseconds
exposure_time_list=[]
for i in range(1,40):
    exposure_time_list.append(exposure_time*i)
exposure_time_array=np.array(exposure_time_list)

#print(exposure_time_array)
file_list=["Switching_Test_200.0cycles_exp0.001s_U2OS_rsEGFP2_25mW488_1mW405
_cell5.csv","Switching_Test_200.0cycles_exp0.001s_U2OS_rsEGFP2_25mW488_2mW4
05_cell5.csv","Switching_Test_200.0cycles_exp0.001s_U2OS_rsEGFP2_25mW488_3m
W405_cell5.csv","Switching_Test_200.0cycles_exp0.001s_U2OS_rsEGFP2_25mW488_4
mW405_cell5.csv","Switching_Test_200.0cycles_exp0.001s_U2OS_rsEGFP2_25mW488
_5mW405_cell5.csv"]

main_dataframe = pd.DataFrame(pd.read_csv(file_list[0]))

for i in range(1,len(file_list)):
    data = pd.read_csv(file_list[i])
    df = pd.DataFrame(data)
    main_dataframe = pd.concat([main_dataframe,df],axis=1)
```

```
Laser_488_power=float(input("Laser_488_power:   ")) # in  milliwatts




y1=main_dataframe.iloc[0:,2]

y2=main_dataframe.iloc[0:,8]

y3=main_dataframe.iloc[0:,14]

y4=main_dataframe.iloc[0:,20]

y5=main_dataframe.iloc[0:,26]

tau_1=[]

tau_2=[]

tau_3=[]

tau_4=[]

tau_5=[]

background1=[]

background2=[]

background3=[]

background4=[]

background5=[]

max_intensity1=[]

max_intensity2=[]

max_intensity3=[]
```

```
max_intensity4=[]
max_intensity5=[]
frac_intensity1=[]
frac_intensity2=[]
frac_intensity3=[]
frac_intensity4=[]
frac_intensity5=[]

def func(x_test,A,tau1,B):
    return A*np.exp(-(x_test)/tau1) + B

for m in range(39):
    index_start = 5+ 50*m + m
    index_stop = index_start -m + 45
    cam_bgr1 =np.average(y1[(index_stop+1):(index_stop+3)])
    cam_bgr2=np.average(y2[(index_stop+1):(index_stop+3)])
    cam_bgr3=np.average(y3[(index_stop+1):(index_stop+3)])
    cam_bgr4=np.average(y5[(index_stop+1):(index_stop+3)])
    cam_bgr5=np.average(y5[(index_stop+1):(index_stop+3)])
    y1_test = y1[index_start:index_stop]-cam_bgr1
    y2_test=y2[index_start:index_stop]-cam_bgr2
    y3_test=y3[index_start:index_stop]-cam_bgr3
    y4_test=y4[index_start:index_stop]-cam_bgr4
```

```
y5_test=y5[index_start:index_stop]-cam_bgr5
x_test=np.arange(len(y1_test))
popt1,pcov=curve_fit(func,x_test,y1_test)
popt2,pcov=curve_fit(func,x_test,y2_test)
popt3,pcov=curve_fit(func,x_test,y3_test)
popt4,pcov=curve_fit(func,x_test,y4_test)
popt5,pcov=curve_fit(func,x_test,y5_test)
A1,tau_frame1,B1 = popt1
A2,tau_frame2,B2=popt2
A3,tau_frame3,B3=popt3
A4,tau_frame4,B4=popt4
A5,tau_frame5,B5=popt5
print('A1:',A1)
print("tau_frame1:",tau_frame1)
print("B1:",B1)
tau1=exposure_time*tau_frame1
print("tau1:",tau1)
background1.append(B1)
tau_1.append(tau1)
y1_fit=func(x_test,A1,tau_frame1,B1)
max_intensity1.append(max(y1_fit))
frac_intensity1.append(B1/(A1+B1))
plt.plot(x_test,y1_test)
```

```
plt.xlabel("x_test")
plt.ylabel("y1_yest")
plt.grid(True)
plt.title("Original Curve")
plt.show()
plt.plot(x_test,y1_fit,'r-',x_test,y1_test,'b:')
plt.xlabel("x_test")
plt.ylabel("y1_fit & y1_test")
plt.grid(True)
plt.title("fitted curve & original together")
plt.show()
print('A2:',A2)
print("tau_frame2:",tau_frame2)
print("B2:",B2)
tau2=exposure_time*tau_frame2
print("tau2:",tau2)
background2.append(B2)
tau_2.append(tau2)
y2_fit=func(x_test,A2,tau_frame2,B2)
max_intensity2.append(max(y2_fit))
frac_intensity2.append(B2/(A2+B2))
plt.plot(x_test,y2_test)
plt.xlabel("x_test")
```

```
plt.ylabel("y2_yest")
plt.grid(True)
plt.title("Original Curve")
plt.show()
plt.plot(x_test,y2_fit,'r-',x_test,y2_test,'b:')
plt.xlabel("x_test")
plt.ylabel("y2_fit & y2_test")
plt.grid(True)
plt.title("fitted curve & original together")
plt.show()
print('A3:',A3)
print("tau_frame3:",tau_frame3)
print("B3:",B3)
tau3=exposure_time*tau_frame3
print("tau3:",tau3)
background3.append(B3)
tau_3.append(tau3)
y3_fit=func(x_test,A3,tau_frame3,B3)
max_intensity3.append(max(y3_fit))
frac_intensity3.append(B3/(A3+B3))
plt.plot(x_test,y3_test)
plt.xlabel("x_test")
plt.ylabel("y3_yest")
```

```
plt.grid(True)
plt.title("Original Curve")
plt.show()
plt.plot(x_test,y3_fit,'r-',x_test,y3_test,'b:')
plt.xlabel("x_test")
plt.ylabel("y3_fit & y3_test")
plt.grid(True)
plt.title("fitted curve & original together")
plt.show()
print('A4:',A4)
print("tau_frame4:",tau_frame4)
print("B4:",B4)
tau4=exposure_time*tau_frame4
print("tau4:",tau4)
background4.append(B4)
tau_4.append(tau4)
y4_fit=func(x_test,A4,tau_frame3,B4)
max_intensity4.append(max(y4_fit))
frac_intensity4.append(B4/(A4+B4))
plt.plot(x_test,y4_test)
plt.xlabel("x_test")
plt.ylabel("y4_yest")
plt.grid(True)
```

```
plt.title("Original Curve")
plt.show()
plt.plot(x_test,y4_fit,'r-',x_test,y4_test,'b:')
plt.xlabel("x_test")
plt.ylabel("y4_fit & y4_test")
plt.grid(True)
plt.title("fitted curve & original together")
plt.show()
print('A5:',A5)
print("tau_frame5:",tau_frame5)
print("B5:",B5)
tau5=exposure_time*tau_frame5
print("tau5:",tau5)
background5.append(B5)
tau_5.append(tau5)
y5_fit=func(x_test,A5,tau_frame5,B5)
max_intensity5.append(max(y5_fit))
frac_intensity5.append(B5/(A5+B5))
plt.plot(x_test,y5_test)
plt.xlabel("x_test")
plt.ylabel("y5_yest")
plt.grid(True)
plt.title("Original Curve")
```

```
    plt.show()
    plt.plot(x_test,y5_fit,'r-',x_test,y5_test,'b:')
    plt.xlabel("x_test")
    plt.ylabel("y5_fit & y5_test")
    plt.grid(True)
    plt.title("fitted curve & original together")
    plt.show()
```

```
plt.plot(exposure_time_array,tau_1,color='red')
plt.plot(exposure_time_array,tau_2,color='blue')
plt.plot(exposure_time_array,tau_3,color='yellow')
plt.plot(exposure_time_array,tau_4,color="green")
plt.plot(exposure_time_array,tau_5,color="purple")
plt.legend(["405:1mW","405:2mW","405:3mW","405:4mW","405:5mW"])
plt.xlabel("exposure time(s)")
plt.ylabel("Time constant in s")
plt.grid(True)
plt.title("Time constant vs exposure time"  + "488:"+str(Laser_488_power)+"mW")
plt.ylim(bottom=0.0)
plt.show()
```

```
plt.plot(exposure_time_array,max_intensity1,color='red')
plt.plot(exposure_time_array,max_intensity2,color='blue')
plt.plot(exposure_time_array,max_intensity3,color='yellow')
plt.plot(exposure_time_array,max_intensity4,color="green")
plt.plot(exposure_time_array,max_intensity5,color="purple")
plt.legend(["405:1mW","405:2mW","405:3mW","405:4mW","405:5mW"])
plt.xlabel("exposure time in s")
plt.ylabel("Max intensity")
plt.grid(True)
plt.title("Max intensity vs exposure time"  + "488:"+str(Laser_488_power)+"mW")
plt.show()

plt.plot(exposure_time_array,background1,color="red")
plt.plot(exposure_time_array,background2,color="blue")
plt.plot(exposure_time_array,background3,color="yellow")
plt.plot(exposure_time_array,background4,color="green")
plt.plot(exposure_time_array,background5,color="purple")
plt.legend(["405:1mW","405:2mW","405:3mW","405:4mW","405:5mW"])
plt.xlabel("exposure time in s")
plt.ylabel("background")
plt.grid(True)
```

```
plt.title("background vs exposure time"  +  "488:"+str(Laser_488_power)+"mW")
plt.show()


plt.plot(exposure_time_array,frac_intensity1,"red")
plt.plot(exposure_time_array,frac_intensity2,"blue")
plt.plot(exposure_time_array,frac_intensity3,"yellow")
plt.plot(exposure_time_array,frac_intensity4,"green")
plt.plot(exposure_time_array,frac_intensity5,"purple")
plt.legend(["405:1mW","405:2mW","405:3mW","405:4mW","405:5mW"])
plt.xlabel("exposure time in s")
plt.ylabel("ratio of background to max intensity")
plt.grid(True)
plt.title("ratio of background to max intensity"  + "488:"+str(Laser_488_power)+"mW")
plt.show()




 # eta = t_read / tau_off

 # read_on = np.exp(-eta *

 p_read) t_read = 0.02

 omega_depl = 0.01
```

```
    d = t_read /
    omega_depl d = i /
    20000
    read_on = 1 / (1 + p_read * d)
    image[i] = read_on * m_on *
    p_read img = img + image[i]


# Activation
NLSIM p_act =
p_off tau_act =
0.02
omega_act = 0.01
g = tau_act /
omega_act g = 0.1
I_on = 1 - np.exp(-p_act * g)


n = 2000
image2 =
np.zeros((n,512,512)) img2
= np.zeros((512,512))
```

```
for i in
    range(n):
    tau_read =
    0.02
    omega_read = 0.01
    h = tau_read /
    omega_read h = i /
    20000
    read_on = 1 / (1 + p_act * h)
    image2[i] = read_on * I_on *
    p_act img2 = img2 + image2[i]


# Saturation
NLSIM p =
p_off
sigma = 0.02
tau = 0.01
kf = 0.5
amp = 2000
```

```
sat_p = (kf * amp*p) / ((1 / (sigma * tau)) +

amp*p) tf.imshow(sat_p)

tf.imsave('sat_p_2000.tif', sat_p)

tf.imsave('sat_p_2000_fft.tif', np.abs(np.fft.fftshift(np.fft.fft2(sat_p))))
```

F. Codes to calculate fluorescence intensity

```
print("40mW data")
import numpy as np
x1=500
a=0.0031544715693731405
A=9.141277590975534
b=2.337523620169604e-33
B=135.38248874548773
Cmax=A+B
C1=(Cmax**-1)*(A*np.exp(-a*x1)+B*np.exp(-b*x1))
print("C1:",C1)
print("Cmax:",Cmax)
#%change
even_change=str(C1*100)+"%"
print("even_change:",even_change)
a=5.864607507362369e-05
A=173.7550715865582
b=0.004702518806352914
B=81.13694204935636
x2=500
Dmax=A+B
D1=(Dmax**-1)*(A*np.exp(-a*x2)+B*np.exp(-b*x2))
print("Dmax:",Dmax)
print("D1:",D1)
odd_change=str((D1*100))+"%"
print("odd_change:",odd_change)
```